CHANGES IN VEGETATION AND ENVIRONMENT OVER THE HOLOCENE

KA‘AU CRATER, O‘AHU, HAWAI‘I

A THESIS SUBMITTED TO THE GRADUATE DIVISION OF THE UNIVERSITY OF HAWAI‘I AT MĀNOA IN PARTIAL FULFILLMENT OF THE REQUIREMENTS FOR THE DEGREE OF

MASTER OF ARTS

IN

GEOGRAPHY

DECEMBER 2012

By

Olivia Schubert

Thesis Committee:

David Beilman, Chairperson
Thomas Giambelluca
Stacy Jorgensen
Henry Diaz

Keywords: paleoclimate, Ka‘au Crater, pollen, Holocene, vegetation

DEDICATION

This is for my mother and my best friend, Susan.

Although you are not here, you are with me every moment of every day.

Thank you for instilling in me a responsibility for the environment, a desire to lead, and reminding me to be kind and compassionate to everyone.

I promise to always do my best for you.

Thank you, Mom.

ACKNOWLEDGEMENTS

First and foremost I would like to express my gratitude to Dave Beilman for the opportunities he has awarded me in the academic setting. Secondly, I'd like to articulate my appreciation to my committee members for their support, valuable feedback, and invaluable patience. I have endless gratitude to my family and friends, of course, for their love and encouragement throughout my academic career. Axel Timmerman, Niklas Schneider and Oliver Timm were instrumental in collecting the soil core from the crater, this research was based on the work they started. Stephanie Pau was crucial to this project, providing reference slides as well as training to me. The Water Resources Research Center at the University of Hawaiʻi supported much of this project, so I am very thankful to them. I have really enjoyed being a part of the Geography Department at the University of Hawaiʻi at Mānoa. Everyone is very supportive of one another, and I have really appreciated this positive atmosphere. Graduate school has been a great experience overall, so I would like to thank everyone who contributed to my journey through aspects such as instruction, support and conversation.
Aloha.

ABSTRACT

Rainfall at three mountaintop locations, two windward: Palolo (Ka'au Crater), Poamoho, and one leeward: Mount Ka'ala, on O'ahu, Hawai'i, was analyzed. Poamoho was found to receive the greatest rainfall monthly and annually, from 1920-2007, followed by Palolo and Mount Ka'ala. Ka'au Crater sits at 460 m elevation in the southern Ko'olau Mountains and at present contains a wetland ecosystem and has accumulated many meters of sediment. At Ka'au Crater, both rainfall and water table level were measured and were greatest between November and March. Rainfall and water table level were found to have a significant relationship. A 4.5 m sediment core retrieved from the crater dating through the Holocene, with seventeen ^{14}C dates, contains fossil pollen including Malvaceae, a dry indicator, and wet-indicator taxa such as Arecaceae *Prichardia*. The precipitation reconstruction derived from the pollen stratigraphy shows a drier early Holocene and a relatively wetter mid to late Holocene.

TABLE OF CONTENTS

LIST OF TABLES

LIST OF FIGURES

CHAPTER 1. GENERAL INTRODUCTION

1.1 Hawaiian flora: past and present

Hawai'i is a lush and beautiful place where the diversity of vegetation is determined by its volcanic origins, isolation, dispersal, evolution and speciation, topography, soil, and climate. The Hawaiian Islands began forming approximately 86 million years ago by means of a hotspot in the oceanic crust. The youngest Hawaiian Islands vary in elevation from sea level to 4205 m (13,796 ft), and range in age from 5 million years old, Kaua'i, to Hawai'i Island, which began forming approximately 600,000 years ago (Monroe and Wicander 1992; Juvik et al. 1998) and is still erupting. It is believed that the islands formed as the Pacific Plate moved in a northwestern direction over the hot spot. The most northwestern islands in the archipelago are therefore the oldest, progressing to the youngest islands in the southeastern portion of the island chain. The islands comprising the main inhabited island chain are shield volcanoes, characteristic of multiple, slow flowing eruptions producing basaltic rock formations (Anderson and Redfern 1987). The present shapes of the islands are the result of hundreds of thousands and millions of years of erosion as well as massive landslides.

Climate in the main Hawaiian Islands is controlled by four factors: latitude, the Pacific Ocean, atmospheric circulation and topography (Sanderson 1993). The main Hawaiian Islands are located just south of the Tropic of Cancer, between 19° 34'-22° 05' N and 155° 20'-160° 10' W, and thus experience relatively small changes in day length and temperature throughout the year. The longest summer day is about 13 hours while the shortest winter day is about 11 hours (Ziegler 2002). The marine influence on climate in the islands is great, and because of their small size the marine influence is felt everywhere (Sanderson 1993). O'ahu is the third largest of the main Hawaiian Islands with are area of 1564 km^2 (604 mi^2) and is formed by the remnants of two elongated shield volcanoes which have eroded to form the Ko'olau and Waianae Mountain ranges on the eastern and western sides of the island respectively (Nichols et al. 1996). The large mountains alter marine effects and lead to marked contrasts in climate between the windward and leeward slopes (Sanderson 1993). Climate throughout the islands is diverse, for example four of the five

Köppen Climate types exist throughout the main Hawaiian Islands: tropical, dry, mesothermal and polar, while all of these but polar are found on Oʻahu (Lau and Mink 2006). The volcanic source, combined with weathering factors over a long period of time have also supplied Hawaiʻi with tremendous diversity of soils. Ten of the twelve orders of the USDA soil taxonomic system are found in the Hawaiian Islands, which contributes to an intriguing assemblage of vegetation (Deenik and McClellan 2007).

Before humans arrived to Hawaiʻi, plants journeyed to the islands via wind, water and birds. An estimated three-quarters of Hawaiian plant colonizers were carried by birds (Kay 1972). Many of these colonizers were very successful owing to a lack of competition. Extraordinary variety and close proximity of contrasting environmental conditions on the Hawaiian Islands probably offered diverse opportunities to particular variants and descendant lineages (Stuessy and Ono 1998). Today there are approximately 1000 native plants in Hawaiʻi, of which approximately 89 percent are endemic (Wood and Dahlquist 2005).

1.2 Objectives of research

Many islands in the Pacific are experiencing increasing human populations, putting stress on natural resources such as the fresh water supply (Chu 1994). Effects of global climate change are also becoming apparent in terms of interannual and spatial rainfall variation. Diaz et al. (2005) documented a reduction in rainfall across more than 100 climate stations in Hawaiʻi over the last 20 years. Giambelluca et al. (2008) found greater surface warming at elevations above 800 m across the Hawaiian Islands during the past 85 years. These changing variables put pressure not only on the unique ecosystems of the Hawaiian Islands (Elison Timm et al. 2011), but the conservation and natural resource leaders unto whom these issues fall most heavily. Crausbay and Hotchkiss (2012) found a strong relationship between vegetation and climate, and projected that climate changes will influence vegetation over time. Much has been learned about rainfall and drought-producing circumstances at mountaintop locations in Hawaiʻi (Giambelluca et al. 2011; Diaz and Giambelluca 2012); however, there is more to be learned about rainfall across mountaintop locations on O‘ahu. The research presented here is focused on addressing two questions concerning rainfall (addressed in Chapter 2), and two questions regarding Holocene vegetation and drought at Ka‘au Crater (Chapter 3).

Question 1 (Chapter 2): Is Ka‘au Crater representative of rainfall trends across mountaintop locations on O‘ahu?

Question 2 (Chapter 2): What are the relationships between El Niño Southern Oscillation (ENSO), the Pacific Decadal Oscillation (PDO) and mountaintop rainfall at windward vs. leeward locations?

> **Hypothesis 2:** Rainfall at Ka‘au Crater and Poamoho will not reflect negative phases of ENSO and PDO as strongly as Mount Ka‘ala due to their windward locations; Ka‘au Crater will have a stronger relationship with PDO phase-changes than Poamoho as it is lower in elevation .

Question 3 (Chapter 3): What were vegetation community composition dynamics in and near Ka‘au Crater, O‘ahu, a mountain wetland, during the Holocene?

> **Hypothesis 3:** A wide variety of plants existed in high elevations during the past 10,000 years including those best suited for precipitation ranges of dry (i.e. Chenopodiaceae), dry-mesic (i.e. Rubiaceae), mesic-wet (i.e. Urticaceae), wet (i.e. Rutaceae) and dry-wet (i.e. Myrsinaceae). Uchikawa et al. (2010) recorded an expansion of C_4 plants from 10,000-6000 cal yrs BP suggesting a reduction in water availability; therefore, it follows that vegetation best-suited for dry, dry-mesic, and mesic were more abundant during this 4,000-year time-span than mesic-to-wet and wet-tolerant plants.

Question 4 (Chapter 3): Have there been long periods with multiple extensive droughts on the island of O‘ahu during the Holocene?

Hypothesis 4: Pollen from abundant dry-tolerant plants, such as Rubiaceae (tree/shrub species), Santalaceae (sandalwood), and Polypodiaceae (terrestrial and epiphytic ferns) have increased and sustained higher abundances for periods of a few hundred years or longer in Ka'au Crater.

1.3 Pacific climate

The Pacific Ocean covers more than a third of the Earth's surface with an area of about 165 million square kilometers, and contains more than half of the Earth's water. Considering its immense size, comprising an area larger than the total land area of the world, the ocean-atmosphere interactions in the Pacific Ocean have effects on weather patterns globally. An important step towards understanding past climate, the main goal of this thesis, is to explore current weather patterns. It is well understood that the mean global air temperature, as well as the mean sea surface temperature and sea level are rising as the global energy content continues to climb (IPCC 2007). Variation and change is inherent in Earth's climate system, as a result of both internal variability within the climate system and external factors (both natural and anthropogenic); however, a topic of common interest is whether, where, and when the Earth has ever experienced changes on the order of those recorded in the past two hundred years. Keeling et al. (2005) documented increasing carbon dioxide levels at Mauna Loa (3400 m) beginning in 1957. Current carbon dioxide levels are 25-35% higher than pre-industrial levels and higher than they have been over the last 100,000 years, since the last interglacial (Stauffer et al. 1984; Barnola et al. 1983; Chen and Millero 1979; Petit et al. 1999; Indermühle et al. 1999). Positive radiative forcing alters the climate system and is largely influenced by anthropogenic activity especially noted since the large and increasing growth in anthropogenic emissions during the Industrial Era (IPCC 2001).

Many uncertainties exist in the realm of climate change in terms of severity and imminence, which makes for a surplus of questions to investigate. One important question is how extreme events, such as droughts, floods, and storms will change in years to come in terms of frequency and severity. Hawai'i is an attractive location to investigate these questions in terms of the Pacific region, as it is the most isolated island chain of comparable size and topographic diversity in the world experiencing a wide variety of weather patterns in the Pacific region (Barbour 2000).

The Intertropical Convergence Zone (ITCZ) is a region of convergence between the northeast and southeast trade winds, where upwelling occurs over much of the equatorial Pacific (Rohli and Vega 2008; Harrison 1990). The ITCZ is a zone of low pressure and ascending air, and appears as a band of clouds consisting of showers, with occasional thunderstorms, that encircles the globe near the equator (Gornitz 2009). The ITCZ moves north during the northern hemisphere's (southern hemisphere's) summer (winter), when the altitude of the sun is then higher in the Northern Hemisphere, and south during the northern hemisphere's (southern hemispheres) winter (summer). The shifting of the ITCZ results in a characteristic latitudinal pattern of distribution of rainy and dry seasons in tropical and subtropical regions (Purves 2001). The seasonal shift is exaggerated over the continents; hence, since the greater amount of the Earth's land mass is in the Northern Hemisphere the average position of the ITCZ is a few degrees north of the equator (Gornitz 2009). It has been suggested that the ITCZ has been dynamic over millennia as well as on century time-spans (Haug et al. 2001; Sachs and Myhrvold 2011).

The ITCZ never migrates over the main Hawaiian Islands; however, the circulation driven by the ITCZ results in the Hadley cell, which does affect the Hawaiian climate. The Hadley cell consists of air rising from the equatorial low-pressure area flowing north and south then descending between 20° and 35° North and South of the equator (subtropical high-pressure cells) (Diaz and Bradley 2004; Juvik and Juvik 1998). Dry air is characteristic of this zone and surface air diverging from the cell generates Earth's trade winds and westerlies. Trade winds in Hawai'i occur approximately 90% of the time during summer, and 50% of the time during winter (Garza et al. 2012; Oliver 2005). The orographic lifting of the trade winds accounts for much of the precipitation received on the windward sides and mountain tops of the Hawaiian Islands; accordingly summertime, May to October, is usually dry over much of the islands while wintertime, November to March, is rainy (Chu and Chen 2005). When the trade winds are interrupted by midlatitude frontal systems, Kona storms result bringing moderate rainfall to the Hawaiian Islands (Chu and Chen 2005).

El Niño Southern Oscillation is a major source of global interannual climate variability (Rein et al. 2005; Philander 1990), specifically ocean/atmosphere heat exchanges, changes in the trade winds, atmospheric circulation, precipitation, and associated atmospheric heating in the Pacific mid-latitudes. It was termed 'El Niño' because of its typical arrival during Christmas or the coming of the 'Christ-child' in Christian religions. Southern Oscillation refers to a pressure signal, observed as a 'seesaw' between the southeastern tropical Pacific and the Australian-Indonesian region, such that when pressure is below normal in one region it tends to be above normal in the other on time scales ranging from monthly to annually (Diaz and Markgraf 1992).

El Niño is a large scale weather pattern involving an anomalously deep Aleutian low and warming of sea-surface temperatures in the eastern and central equatorial Pacific which result in an increase in convection and relocation of the ITCZ and also entails abnormal hydrologic patterns, coastal upwelling and storm events between the eastern and western Pacific Ocean (Chu 1994; Chu and Chen 2005; IPCC 2007). Warming of the entire equatorial Pacific eastward of 170°E increases to a maximum during an El Niño year around December which correlates with a partial or complete collapse of the sea-level pressure gradient across the tropical South Pacific (Diaz and Markgraf 1992). El Niño recurs on a time scale of two to eight years (Chu and Chen 2005). Kirov and Georgieva (2002) suggested that the intensity and occurrence frequency of El Niño are also affected by solar output, thus lessening at secular solar maximum and heightening at secular solar minimum. La Niña is the complementary phase to El Niño and is associated with low sea surface temperatures near the equator and stronger than normal trade winds, which push the ocean water away from the equator in each hemisphere allowing for cold water to rise and replace the warm water (Philander 1990). La Niña is often referred to as the cold phase of ENSO and El Niño as the warm phase of ENSO and occurs almost as often as El Niño (Philander 1990).

El Niño may cause droughts, floods, monsoon failures, and changes in marine ecosystems among other altered marine and terrestrial conditions. During an El Niño year, the western portion of the Northeast Pacific basin near Hawai'i experiences more tropical cyclone genesis, changing the typical trade wind pattern and increasing the prevalence of warm south winds (Landsea 2000). The warm ocean temperatures and altered wind patterns often lead to drought in the winter months followed by large and intense storms and possibly hurricanes during the rest of the year (Ropelewski and Halpert 1987). La Niña conditions usually produce wetter winters (December-February) on O'ahu (Philander 1990; Diaz and Giambelluca 2012).

Trenberth and Stepaniak (2001) found a shift since the mid-1970s to generally above-normal SSTs in the eastern and central equatorial Pacific and a tendency towards a more prolonged and stronger El Niño. Multi-model averages show a weak shift towards average background conditions which may be described as 'El Niño-like', with sea surface temperatures (SSTs) in the central and east equatorial Pacific warming more than those in the west, weakened tropical circulations and an eastward shift in mean precipitation (IPCC 2007). Trenberth and Stepaniak (2001) predicted that the extremes of the hydrological cycle such as floods and droughts, common with ENSO, are apt to be enhanced with global warming.

The Pacific Decadal Oscillation (PDO) is a pan-Pacific climate phenomenon that involves interdecadal climate variability in the tropical pacific and a coupled ocean-atmosphere mode of variability occurring every 20-30 years (Mantua and Hare 2002). Using regional patterns of the PDO between December and February, Mantua et al. (1997) found that the PDO has a negative correlation with Hawai'i winter rainfall; during a positive PDO phase PDO, the linear association is about -40 mm for a PDO value of +1. During a positive PDO phase, sea level pressures are below average over the North Pacific, whereas they are above average during a negative PDO phase (Barron and Anderson 2011). A positive PDO phase resembles El Niño-like North American temperature and precipitation anomalies and involves a strengthened Aleutian Low, while a negative PDO phase is more similar to La Niña-like climate patterns with a weak Aleutian Low (Mantua et al. 1997).

The Aleutian Low is defined as a semi-permanent, subpolar area of low pressure located in the Gulf of Alaska near the Aleutian Islands which is a generating area for storms a location where migratory lows often reach maximum intensity (Schneider et al. 1996). Active in the cold part of the year in the Northern Hemisphere, the Aleutian Low is on average located at a latitude of about 52.5°N and a longitude of about 176°E (Kirov and Georgieva 2002). The Aleutian low is associated with the large-scale, low frequency mean flow or stationary wave patterns in the general circulation of the Northern Hemisphere (Overland et al. 1999). A positive (negative) PDO phase is associated with a strengthened (weakened) Aleutian Low. The Aleutian Low is strengthened and/or located farther to the east during a positive PDO phase and weakened and/or located more to the west during a negative PDO. During winter months in the Northern Hemisphere, the Aleutian Low is located farther south and commonly produces extra-tropical storms, which hit the western United States and Alaska. The consequences of these storms materialize in Hawai‘i in the form of high ocean waves reaching the northern shores of the main islands during the winter months (Ziegler 2002).

The North Pacific High (NPH) is another semi-permanent center of action in the Northern Pacific. This large region of high surface pressure is most pronounced during the summer time in the Northern Hemisphere and is located at an average latitude and longitude of 33.5°N and 203°E (Kirov and Georgieva 2002). In Hawai‘i, when the Aleutian low is stronger, sea level is high, the NPH is weaker, and there is a slight weakening of the northeast trade winds (Firing et al. 2004). When the Aleutian Low is weaker, the opposite conditions occur. Kirov and Georgieva (2002) found a correlation between solar activity and these North Pacific pressure patterns in that the longitude of the Aleutian Low decreases with increasing solar activity (it moves to the West) while the longitude of the NPH increases (moves to the East).

The Pacific Ocean and the continents bordering it clearly undergo immense and comprehensive climatic patterns. It has been predicted that many of these patterns will alter as time progresses; therefore, gaining insight on current as well as paleoclimatic conditions is advantageous in forecasting and preparing for future events (IPCC 2007).

1.4 Pacific climate during the Holocene

Long-term climate records display pre-industrial environmental conditions and also help to reveal human impacts on the environment as well as increase our knowledge of global climatic changes. Considering the isolation of Hawaiʻi, it is useful and sometimes necessary to use records capturing climate variability throughout the Pacific to infer climate patterns in the Hawaiian Islands. Hodell et al. (1991) found that orbitally-driven changes in the mean meridional positioning of the ITCZ during the Holocene caused significant changes in the hydrologic cycles in regions where precipitation is either directly influenced by the ITCZ itself, or by seasonal monsoons modulated by the ITCZ. Using a high-resolution nested climate model, Diffenbaugh et al. (2006) reported a reduction of summer precipitation over the central continental United States and northern Rocky Mountains between 8000 and 4000 cal yr BP following reduced summer insolation compared to the early Holocene, which coincides with widespread drought in the interior western North America. Moy et al. (2002) suggested that the intensity and occurrence of El Niño was low during the early Holocene, increased since about 7000 cal yr BP, and was particularly strong around 5000 cal yr BP and after 2000 cal yr BP. Clement et al. (2000) proposed insolation-driven suppression of ENSO warm events during the middle Holocene and increased ENSO strength and variability during the late Holocene. Still further proxy records in the northeastern Pacific and adjacent coastal regions of North America indicated stepwise increases in ENSO warm event variability and strength at 4200, 3000, and 2000 cal yr BP (Barron and Anderson 2011). Barron and Anderson (2011) suggested that a pattern of wetter conditions in the Pacific Northwest (Oregon and Washington) approximately 6000-4000 cal yr BP and drier conditions in the southwest U.S. are suggestive of a generalized negative PDO (similar to La Niña-like conditions) phase in the North Pacific. They concluded that the mid-Holocene was marked by suppressed expression of positive PDO and El Niño then transitioned into a more positive PDO-like North Pacific after ~3500 cal yr BP. Also consistent with a negative mid-Holocene PDO phase, Heusser et al. (1985) found precipitation on the southeast Alaskan coast was reduced by an estimated 30-50% between 8000 and 5000 cal yr BP perhaps resulting from a weaker Aleutian Low.

Paleoclimatic trends in equatorial and Southern Hemisphere locations are also valuable in deciphering climatic patterns Hawai'i and the northern Pacific region. Pollen records from Lakes Zempoala and Quila (19° 3' S, 99° 18' W) located southwest of Mexico City, Mexico indicate warmer and drier conditions than at present from 6320 to 2540 cal yr BP (Almeida-Lenero et al. 2005). In partial agreement with Barron and Anderson (2011), Rein et al. (2005) demonstrated in higher resolution lithologic records from the El Niño region off the coast of Peru, robust El Niño signals (in terms of intensity and/or frequency) after 5000 cal yr BP. Furthermore, Lake Titicaca (32° 39' S, 70° 0' W), located in the Andes Mountains on the border of Peru and Bolivia, was found to be characterized by a dry episode with the lowest water level recorded in 30,000 years during the mid-Holocene between 8000 and 5000 cal yr BP (Abbott et al. 2003).

Additional records from South America show that between 8000 and 5000 cal yr BP the eastern Pacific and western portion of South America became moister, while at the same time northeastern South America became drier, indicative of El Niño-like precipitation patterns (McGlone et al. 1992). McGlone et al. (1992) found amplified variability in records in the form of an enlarged degree of change in lake level as well as an 'anomalous' combination of plant assemblages after 5000 cal yr BP. From this they suggested increased moisture and drought and proposed that repeated occurrences of ENSO events could result in such records. Concurrently, flood deposits in coastal Peru and El Niño-type strandlines in southeastern Brazil also point to increased frequency of ENSO events (McGlone et al. 1992). On the contrary, a pollen record from the highlands of the western Andean Cordillera in southern Peru shows more moist and cold conditions compared to present day from the early to mid Holocene, 9700-5200 cal yr BP, and drier climatic conditions between 5200 and 3000 cal yr BP (Kuentz et al. 2011). Kuentz el al. (2011) attributed the former climate with La Niña-like conditions, and linked the latter drier climate with precession cycles, the southward displacement of the ITCZ, as well as the increase in El Niño frequencies observed during this period.

Moving westward over the Pacific Ocean, paleoclimatic early Holocene records from Australasia suggest generally drier conditions, which are consistent with the southern oscillation being in a more negative phase (McGlone et al. 1992). McGlone et al. (1992) suggested that it appears improbable that the ENSO system was operating as it is now during the early Holocene. This conclusion was based on lake and soil profiles from Australia not exhibiting widespread or intense disturbance of the landscape.

It is clear that weather patterns in the Pacific are far-reaching and diverse. By linking similar patterns across locations, insight may be gained about areas that are less studied. Therefore, because the tropical/subtropical Pacific Ocean represents an enormous source of heat, moisture, as well as an important zone in terms of atmospheric pressure and wind patterns, reliable proxy records from oceanic locations in the Pacific are particularly valuable and much needed in the context of paleoclimatology (Uchikawa et al. 2010). The Hawaiian Islands provide a different perspective on Pacific-wide climate patterns than coastal locations surrounding the Pacific Ocean, therefore expanding paleoclimate records throughout the islands is much needed.

1.5 Modern climate in Hawai‘i

The Hawaiian Islands are located in the sub-tropical high-pressure zone impacted by the descending flow of the Hadley circulation. The interactions between the island topography and the general circulation patterns produce a spatially heterogeneous climate pattern (Elison Timm et al. 2011). Northeasterly trade winds in the lower atmosphere are predominant and cause orographic rainfall year round, making mountain areas generally wetter than sea-level areas (Lyons 1982). The winter or wet season is characterized by extratropical cyclonic disturbances, which cause increased rainfall (Schroeder 1993). Due to the small size of the individual islands, no inland area is very far from the ocean; therefore, the marine effect is felt everywhere, as a result temperature variations are somewhat modest. The average year-round temperature is about 24° C (75° F), the average temperature of August, the warmest month is 25.8° C (78.4° F) and the average temperature for the coolest month, February, is 22.2° C (72.0° F) (Schroeder 1993; Ziegler 2002).

In recent years, Chu and Chen (2005) reported a decrease in rainfall in Hawaiʻi since the early 1900s. Diaz et al. (2005) created a rainfall index for Hawaiʻi using 100 climate stations having lengthy records and found a marked decline in rainfall over the last 20 years. They remarked that this decrease agrees with the mid-1970s climate change in the Pacific and furthermore, may be the result of an anomalous sinking motion related to changes in the Hadley circulation (Meehl et al. 2008). Giambelluca et al. (2008) documented secular temperature changes in the Hawaiian Islands for the past 85 years based on an index using 21 stations. Their results show a relatively rapid rise in surface temperature in the last 30 years, with stronger warming at the higher elevations. Higher elevation stations, above 800 m, warmed by a factor of about three (0.27° C/decade), while lower sites warmed 0.09° C/decade since 1975.

Effects of climate change are important to monitor at mountain locations as temperature change may have large consequences for native biodiversity, water resources and carbon sequestration (Arnell 1999; Diaz and Graham 1996; Crausbay and Hotchkiss 2010; Kappelle et al. 1999; Litton and Giardina 2008). Temperatures at high elevations are projected to increase with increasing elevation (Bradley et al. 2004). Atmospheric carbon dioxide (CO_2) concentrations were documented to have increased by nearly 70 parts per million (ppm) from approximately 320 ppm in 1960 to 390 ppm in 2010 at the Mauna Loa Observatory on the island of Hawaiʻi (Keeling and Whorf 2005). Levels of atmospheric CO_2 are predicted to increase in the future, but the extent of increase is uncertain. Carbon dioxide fertilization effects are also of concern. Studies have shown that increased amounts of CO_2 results in a persistent fertilization effect on net ecosystem carbon sequestration over time; furthermore, fertility can restrain the response of carbon sequestration to increased atmospheric CO_2 (Oechel et al. 1994; Oren et al. 2001).

In Hawaiʻi, the steep topographic gradients are a specific area of interest in terms of climate change because they are responsible for the complex pattern of rainfall and vegetation zones which are characterized by very short horizontal and vertical scales (Elison

Timm et al. 2011). Mountain rain is the crucial component of groundwater recharge in the Hawaiian Islands, for that reason it is necessary to investigate the organic geochemical and vegetation history of mountain locations to better understand the intensity and frequency of dry climate periods in Hawaiʻi.

1.6 Hawaiʻi climate during the Holocene

Hawaiʻi has become a hub for climate change research owing to its ecosystem diversity, the existence of numerous climate zones, and the long-term carbon dioxide records from the Mauna Loa Observatory. Although studies concerning the present and modeling future climate scenarios are prevalent, this is not the case for paleoclimate records. While much research encompasses reef cores and observations at low elevations and notable advancements have been made in paleoclimate of high elevations of the Hawaiian Islands, gaps remain to be filled.

Uchikawa et al. (2010) found an increase in the $\delta^{13}C$ values of leaf wax n-alkanes in an analysis of sediment from Ordy Pond in dry southwest Oʻahu around the mid-Holocene, approximately 5000 cal yr BP. This was interpreted as a shift in the relative abundances of C_3 (primarily trees and shrubs) to C_4 species (mostly grasses) in response to decreased water availability due to reduced wintertime precipitation perhaps associated with El Niño-like conditions. Burney et al. (1995) investigated a sediment core from a high-elevation bog on Maui, and found drier conditions between 9400-5800 cal yr BP, wetter conditions between 5800-2200 cal yr BP and a variable late Holocene. Hotchkiss and Juvik (1999) produced a pollen record from a soil core from Kaʻau Crater, Oʻahu dating approximately 25,860 to 8120 cal yr BP. The uppermost portion of their record spans the early Holocene and records warm conditions and low moisture.

Hotchkiss and Juvik (1999) postulated that large changes in Quaternary sea level position affected rainfall. Fluctuations in relative Holocene sea levels reflect fundamental geodynamic processes and are of interest for forecasting future environmental conditions along island shorelines (Dickenson 2001). The timing of considerable sea-level change following the glacial low stand occurred much earlier than the Holocene, however, Stearns

(1977) and Grossman & Fletcher (1998) showed the existence of a Holocene highstand, approximately 1-2 meters above modern mean sea level 3500 cal yr BP on Oʻahu. Fluvial, marine, and mixed fluvial-marine deposition on the coastal plain of Hanalei Bay on the north shore of Kauaʻi, Hawaiʻi taken by Calhoun and Fletcher (1996) record a middle- to late-Holocene fall of relative sea level. Their record indicates a seaward shift of the shoreline beginning at least 4800–4580 cal yr BP and continuing until at least 2160–1940 cal yr BP. Recent observations of reef accretion by Rooney et al. (2004) suggest that a change in wave energy contributed to the reduction or termination of Holocene reef accretion by 5000 cal yr BP in some high-energy windward shores of Oʻahu, Kauaʻi and Molokaʻi. They propose that the shift from the early Holocene weak ENSO conditions to enhanced ENSO initiating around 5000 cal yr BP may aid in explaining patterns of reef accretion in Hawaiʻi.

In this thesis, I commence with an investigation of recent rainfall trends at three mountain top locations on Oʻahu. I then present a vegetation reconstruction of Kaʻau Crater derived from fossil pollen extracted from a sediment core. The four questions addressed in this thesis aim to frame paleoclimatic data with respect to current weather patterns with an objective to better understand atmospheric circulation changes over long periods of time; and furthermore, to better understand how vegetation communities adjust to climatic shifts.

1.7 Literature cited

Abbot, M.B., Wolfe, B.B., Seltzer, G.O., Aravena, R., and Mark, B.G. 2003. Holocene paleohydrology and glacial history of the central Andes using multiproxy lake sediment studies. *Palaeogeography, Palaeoclimatology, Palaeoecology* 194, 123-138.

Almeida-Lenero, L., Hooghiemstra, H., Cleed, A.M., and van Geel, B. 2005. Holocene climatic and environmental change from pollen records of lakes Zempoala and Quila, central Mexican highlands. *Review of Palaeobotany and Palynology* 136, 63-90.

Anderson, I., and Redfern, M. 1987. Hawai'i: a picture window on the Universe. *New Scientist* 30 46-50.

Arnell, N.W. 1999. Climate change and global water resources. *Global Environmental Change* 9, 531-549.

Barbour, Michael G. *North American terrestrial vegetation*. 2nd ed. Cambridge University Press, 2000. Print.

Barnola, J.M., Raynaud, D., Neftel, A., and Oeschger, H. 1983. Comparison of CO_2 measurements by two laboratories on air from bubbles in polar ice. *Nature* 303, 410-413.

Barron, J.A., and Anderson, L. 2011. Enhanced Late Holocene ENSO/PDO expression along the margins of the eastern North Pacific. *Quaternary International* 235, 3e12.

Bradley, R.S., Keimig, F.T., and Diaz, H.F. 2004. Projected temperature changes along the American cordillera and planned GCOS network. *Geophysical Research Letters* 31, L16210, 4 pp.

Burney, D.A., DeCandido, R.V., Burney, L.P., Hostel-Hughes, F.N., Stafford Jr., T.W., and James, H.F. 1995. A Holocene record of climate change, fire ecology and human activity from montane Flat Top Bog, Maui. *Journal of Paleolimnology*, 13.3.

Calhoun, R.S., and Fletcher, C.H. 1996. Late Holocene coastal-plain stratigraphy and sea-level history at Hanalei, Kaua'i, Hawaiian Islands. *Quaternary Research* 45, 47–58.

Christopherson, Robert. "Atmosphere and Oceanic Circulations." *Elemental Geosystems.* Sixth ed. Upper Saddle River: Pearson Education, Inc., 2010. 123. Print.

Chen, C.T.A., and Millero, F.J. 1979. Gradual increase of oceanic CO_2. *Nature* 277, 305-307.

Chu, P.-S. 1994. Hawai'i Rainfall Anomalies and El Niño. *Journal of Climate* 8, 1697-1703.

Chu, P.-S., and Chen, H. 2005. Interannual and Interdecadal Rainfall Variations in the Hawaiian Islands. *Journal of Climate* 18, 4796-4813.

Clement, A.C., Seager, R., and Cane, M.A. 2000. Suppression of El Niño during the mid-

Holocene by changes in the Earth's orbit. Paleoceanography 15, 731e737.

Crausbay, S.D., and Hotchkiss, S.C. 2010. Strong relationships between vegetation and two perpendicular climate gradients high on a tropical mountain in Hawaiʻi. *Journal of Biogeography* 37, 1160-1174.

Crausbay, S.D., and Hotchkiss, S.C. 2012. Pollen-vegetation relationships at a tropical cloud forest's upper limit and accuracy of vegetation inference. *Review of Palaeobotany and Palynology* 184, 1-13.

Deenik, J., and McClellan, A.T. 2007. Soils of Hawaiʻi. *Soil and Crop Management*. Cooperative Extension Service, College of Tropical Agriculture and Human Resources, University of Hawaiʻi at Mānoa.

Diaz, H.F., and Bradley, R.S. (eds.). *The Hadley circulation: present, past and future*. Dordrecht: Kluwer academic publishers, 2004. Print.

Diaz, H.F., Chu, P.-S., and Eischeid, J.K., 2005. Rainfall changes in Hawaiʻi during the last century. In: 16th Conference on Climate Variability and Change. American Meteorological Society, San Diego, California.

Diaz, H.F., Giambelluca, T.W., Changes in Atmospheric Circulation Patterns Associated with High and Low Rainfall Regimes in the Hawaiian Islands Region on Multiple Time Scales, *Global and Planetary Change* (2012),doi: 10.1016/j.gloplacha.2012.08.011

Diaz, H.F., and Graham, N.E. 1996. Recent changes in tropical freezing heights and the role of sea surface temperature. *Nature* 383, 152 – 155.

Diaz, H.F., and Markgraf, V. (eds.). *El Niño: historical and paleoclimatic aspects of the southern oscillation*. Cambridge England: Cambridge University Press, 1992. Print.

Dickinson, William R. 2001. Paleoshoreline record of relative Holocene sea levels on Pacific islands. *Earth-Science Reviews* 55, 191-234.

Diffenbaugh, N.S., Ashfaq, M., Shuman, B., Williams, J.W., and Bartlein, P.J. 2006. Summer aridity in the United States: Response to mid-Holocene changes in insolation and sea surface temperature. *Geophysical Research Letters*, 33.

Elison Timm, E., Diaz, H.F., Giambelluca, T.W., and Takahashi, M. 2011. Projection of changes in the frequency of heavy rain events over Hawaiʻi based on leading Pacific climate modes. *Journal of Geophysical Research* 116, D04109.

Firing, Yvonne L., Merrifield, Mark A., Schroeder, Thomas A., and Qiu, Bo. 2004. Interdecadal Sea Level Fluctuations at Hawaiʻi. *Journal of Physical Oceanography* 34, 2514-2524.

Garza, Jessica A., Chu, Pao-Shin, Norton, Chase W., and Schroeder, Thomas A. 2012 Changes of the prevailing trade winds over the islands of Hawaii and the North Pacific. Journal of Geophysical Research 117, D11109.

Giambelluca, T.W., Chen, Q., Frazier, A.G., Price, J.P., Chen, Y.-L, Chu, P.-S., Eischeid, J., and Delparte, D. (2011). The Rainfall Atlas of Hawai'i.

Giambelluca, T.W., Diaz, H.F., and Luke, M. 2008. Secular temperature changes in Hawai'i. *Geophysical Research Letters*, 35, L12702.

Gornitz, V.. *Encyclopedia of paleoclimatology and ancient environments*. Dordrecht, Netherlands: Springer, 2009. Print.

Grossman, E.E., and Fletcher III, C.H. 1998. Sea level higher than present 3500 years ago on the northern main Hawaiian Islands. *Geology* 26, 363-366.

Harrison, Craig S. *Seabirds of Hawai'i: natural history and conservation*. Ithaca, N.Y.: Comstock Pub. Associates, 1990. Print.

Haug, G.H., Hughen, K.A., Sigman, D.M., Peterson, L.C., and Röhl, U. 2001. Southward Migration of the Intertropical Convergence Zone Through the Holocene. *Science* 293(5533), 1304-1308.

Huesser, C.J., Huesser, L.E., and Peteet, D.M. 1985. Late-Quaternary climatic change on the American North Pacific Coast. *Nature* 315, 485-487.

Hodell, D., Curtis, J., Jones, G., Higuera-Gundy, A., Brenner, M., Binford, M., and Dorsey, K. 1991. Reconstruction of Caribbean climate change over the past 10500 years. *Nature* 352, 790-793.

Hotchkiss, S., and Juvik, J.O. 1999. A late-Quaternary pollen record from Ka`au Crater, O'ahu, Hawai`i. *Quaternary Research* 52, 115-128.

Indermühle, A., Stocker, T.F., Joos, F., Fischer, H., Smith, H.J., Wahlen, M., Deck, B., Mastroianni, D., Tschumi, J., Blunier, T., Meyer, R., and Stauffer, B. 1999. Holocene carbon-cycle dynamics based on CO_2 trapped in ice at Taylor Dome, Antarctica. *Nature* 398, 121-126.

Intergovernmental Panel of Climate Change, edited by J.T. Houghton et al., Cambridge Univ. Press, Cambridge, U. K. IPCC, 2001: *Climate Change 2001: The Scientific Basis. Contribution of Working Group I to the Third Assessment Report of the Intergovernmental Panel on Climate Change* [Houghton, J.T., Y. Ding, Griggs D.J., Noguer, M., van der Linden, P.J., Dai, S., Maskell, K., Johnson, C.A. (eds.)]. Cambridge University Press, Cambridge, United Kingdom and New York, NY, USA.

Intergovernmental Panel on Climate Change, edited by S. Solomon et al., Cambridge Univ. Press, Cambridge, U. K. IPCC, 2007: *Climate Change 2007: The Physical Science*

Basis. Contribution of Working Group I to the Fourth Assessment Report of the Intergovernmental Panel on Climate Change [Solomon, S., Qin, D., Manning, M. Chen, Z., Marquis, M., Averyt, K.B., Tignor, M., and Miller, H.L. (eds.)]. Cambridge University Press, Cambridge, United Kingdom and New York, NY, USA.

Juvik, Sonia P., Juvik, James O., and Paradise, Thomas R. *Atlas of Hawai'i*. 3rd ed. Hawai‘i: University of Hawai‘i Press; 1998. Print.

Kappelle, M., Van Vuuren, M.M., and Baas, P. 1999. Effects of climate change on biodiversity: a review and identification of key research issues. *Biodiversity and Conservation* 8, 1383-1397.

Kay, A.E. *A natural history of the Hawaiian Islands; selected readings*. Honolulu: University of Hawai‘i; distributed by the University Press of Hawai‘i, 1972. Print.

Keeling, C.D., and T.P. Whorf. "Atmospheric CO2 records from sites in the SIO air sampling network." *Trends: A compendium of data on global change* 2009 (2005).

Keuntz, A., Ledru, M.-P., and Thoret, J.-C. 2011. Environmental changes in the highlands of the western Andean Cordillera, southern Peru, during the Holocene. The Holocene. July 22, DOI: 10.1177/0959683611409772.

Kirov, B., and Georgieva, K. 2002. Long-term variation and interrelations of ENSO, NAO and solar activity. *Physics and Chemistry of the Earth* 27, 441-448.

Landsea, C.W. 2000. El Niño/Southern Oscillation and the Seasonal Predictability of Tropical Cyclones. In: El Niño and the southern oscillation: multiscale variability and global and regional impacts. Diaz, H.F., and Markgraf, V. (eds). Cambridge: Cambridge University Press, 2000. 152-155. Print.

Lau, S.L., and Mink, J.F. *Hydrology of the Hawaiian Islands*. Honolulu: University of Hawai'i Press, 2006. Print.

Litton, C.M., and Giardina, C.P. 2008. Below-ground carbon flux and partitioning: global patterns and response to temperature. *Functional Ecology* 22, 941-954.

Lyons, S.W. 1982. Empirical orthogonal function analysis of Hawaiian rainfall. *Journal of Applied Meteorology* 21, 1713-1729.

MacCaughey, Vaughan. 1917. A Survey of the Hawaiian Land Flora. *Botanical Gazette* 64(2), 89-114.

Mantua, N.J., and Hare, S.R. 2002. The Pacific Decadal Oscillation. *Journal of Oceanography*, 58, 35-44.

Mantua, N.J., Hare, S.R., Zhang, Y., Wallace, J.M., and Francis, R.C. 1997. A Pacific Interdecadal Climate Oscillation with Impacts on Salmon Production. *Bulletin of the American Meteorological Society* 78, 1069-1079.

McGlone, M.S., Kershaw, A.P., and Markgraf, Vera. 1992. El Niño/Southern Oscillation climatic variability in Australasian and South American paleoenvironmental records. In: El Niño: Historical and Paleoclimatic Aspects of the Southern Oscillation by Henry F. Diaz and Vera Markgraf. Pg 435-462.

Meehl, Gerald A., Hu, Aixue, and Santer, Benjamin D. 2008. The Mid-1970s Climate Shift in the Pacific and the Relative Roles of Forced versus Inherent Decadal Variability. *Journal of Climate* 22, 780-792.

Monroe, James S., and Wicander, Reed. *Physical geology: exploring the Earth*. St. Paul: West Pub. Co., 1992. Print.

Moy, M., Seltzer, G., Rodbell D., and Anderson, D. 2002. Variability of El Niño/Southern Oscillation activity at millennial timescales during the Holocene epoch. *Nature* 420.

Nichols, W.D., Shade, P.J., and Hunt, C.D. 1996. *Summary of the O'ahu, Hawai'i, Regional Aquifer-System Analysis*. Regional Aquifer-System Analysis, O'ahu, Hawai'i, U.S. Geological Survey Professional Paper 1412-A. U.S. Government Printing Office 1997-545-976.

Oliver, John E. "Tourism and Climate." *Encyclopedia of world climatology*. Dordrecht, Netherlands: Springer, 2005. 732. Print.

Oechel, Walter C., Cowles, Sid, Grulke, Nancy, Hastings, Steven J., Lawrence, Bill, Prudhomme, Tom, Richers, George, Strain, Boyd, Tissue, David, and Vourlitis, George. 1994. Transient nature of CO_2 fertilization in Arctic tundra. *Nature* 371, 500-503.

Oren, R., Ellsworth, D.S., Johnsen, K.H., Phillips, N., Ewers, B.E., Maier, C., Schafer, K.V.R., McCarthy, H., Hendrey, G., McNulty, S.G., and Katul, G.G. 2001. Soil fertility limits carbon sequestration by forest ecosystems in a CO_2-enriched atmosphere. *Nature* 411, 469-472.

Overland, James E., Adams, Jennifer Miletta, and Bond, Nicholas A. 1999. Decadal Variability of the Aleutian Low and its Relation to High-Latitude Circulation. *Journal of Climate* 12, 1542–1548.

Petit, J.R., Jouzel, J., Raynaud, D., Barkov, N.I., Barnola, J.-M., Basile, I., Bender, M., Chappellaz, J., Davis, M., Delaygue, G., Delmotte, M., Kotlyakov, V.M., Legrand, M., Lipenkov, V.Y., Lorius, C., PÉpin, L, Ritz, C., Saltzman, E., and Stievenard, M. 1999. Climate and atmospheric history of the past 420,000 years from the Vostok ice core, Antarctica. *Nature* 399, 429-436.

Philander, George S. *El Niño, La Niña, and the southern oscillation*. San Diego: Academic Press, 1990. Print.

Purves, William K. *Life, the science of biology*. 6th ed. Sunderland, MA: Sinauer Associates, 2001. Print.

Rein, B., Luckge, A., Reinhardt, L., Sirocko, F., Wolf, A., and Dullo, W. 2005. El Niño variability off Peru during the last 20,000 years. *Paleoceanography* 20*, PA4003*.

Rooney, J., Fletcher, C., Grossman, E., Engels, M., and Field, M. 2004. El Niño Influence on Holocene Reef Accretion in Hawai'i. *Pacific Science*, 305-324.

Rohli, Robert V., and Vega, Anthony J. *Climatology*. Sudbury, Mass.: Jones and Bartlett Publishers, 2008. Print.

Ropelewski, C.F., and Halpert, M.S. 1987. Global and Regional Scale Precipitation Patterns Associated with the El Niño/Southern Oscillation. *Monthly Weather Review* 115, 1606-1626.

Sachs, J.P., and Myhrvold, C.L. 2011. A Shifting Band of Rain. *Scientific American* 304(3), 60-65.

Sanderson, Marie. *Prevailing trade winds: climate and weather in Hawai'i*. Honolulu: University of Hawai'i Press, 1993. Print.

Schneider, Stephen Henry, Mastrandrea, Michael, and Root, Terry. "Icelandic Low." *Encyclopedia of climate and weather*. Second Edition ed. New York: Oxford University Press, 1996. 162-164. Print.

Schroeder, T. 1993. Climate controls. In *Prevailing trade winds, climate and weather in Hawai'i*, ed. M. Sanderson, 12-72. Honolulu: University of Hawai'i Press.

Stauffer, B., Siegenthaler, U., and Oeschger, H. 1984. Atmospheric CO_2 concentrations during the last 50,000 y from ice core analysis. *Abstr. AGI Chapman Conf. on Nat. Var. in Carbon Dioxide and the Carbon Cycle, Innisbrook, Tarpon Springs, Fla.*

Stearns, H. S., 1977, Radiocarbon profile of Hanauma Reef, O'ahu, Hawai'i: Discussion and reply: *Geological Society of America Bulletin* 88, p. 1535.

Stuessy, Tod F., and Ono, Mikio. *Evolution and speciation of island plants*. Cambridge: Cambridge University Press, 1998. Print.

Trenberth, K., and Stepaniak, D. 2001. Indices of El Niño Evolution. *Journal of Climate* 14, 1697-1701.

Uchikawa, J., Popp, B., Schoonmaker, J., Timmermann, A., and Lorenz, S. *in press*. 2010. Geochemical and climate modeling evidence for Holocene aridification in Hawai'i:

dynamic response to a weakening equatorial cold tongue. *Quaternary Science Reviews*, doi: 10.1016/j.quascirev.2010.07.014.

Wood, Paul, and Dahlquist, Ron. *Flowers and plants of Hawai'i*. Waipahu, Hawai‘i: Island Heritage Pub., 2005. Print.

Ziegler, Alan C. *Hawaiian natural history, ecology, and evolution*. Honolulu: University of Hawai'i Press, 2002. Print.

CHAPTER 2: TRENDS IN WINDWARD AND LEEWARD MOUNTAIN RAINFALL ON O‘AHU

2.1 Ka‘au Crater rainfall and water table

Rainfall and water table level at Ka‘au Crater were studied over a 13.5-month period to gain a better understanding of present rainfall and conditions in the crater. The closest rainfall station to Ka‘au Crater with up-to-date data is the Hawai‘i Archived Hydronet Data, HI-25 Palolo FS PFSH1 station. Rainfall at the Palolo station is pronounced between December and January, and greatest between March and April (Fig. 1). The water table level parallels the rainfall values, with an average of 3.9 mm per day (Fig. 1). The dry season rainfall average is 2.61 mm per day lower than the wet season average. The Hydronet rainfall station is not located in the actual crater and therefore may not accurately represent the actual Ka‘au rainfall values. Grand and Gaidos (2010) measured rainfall inside Ka‘au Crater for 178 days, then compared the values with data from the same Palolo rain gauge used in this study and found the station in the crater received 25% more rainfall.

Water table level was recorded in Ka‘au Crater from June 9, 2011 until September 29, 2012 using an Odyssey capacitance water level logger with a 0.5 m probe length. Overall, it appears to take moderate rainfall events to raise the water table level. A linear regression of rainfall and water table level in Ka‘au Crater shows a positive relationship and significant p-value of <0.001 and R-squared of 0.0677. The water table level was highest during the 480 day period on March 6, 2012 at 1413 mm and lowest on June 19, 2012 at 871 mm (Fig. 1). The average daily water table level was 1189.5 mm (223 mm below the maximum recorded position). The instances of greatest water table level occurred between November 2011 and March 2012, which is considered the wet or rainy season in Hawai‘i (Chu and Chen 2005). The lowest persisting water table level occurred during the beginning of the summer, from the end of May 2012 to July 2012, which is during the dry season. Another period of low water table level happened uncharacteristically during the wet season, from early January 2011 to the first week in February 2012. This phenomenon is consistent with the long-term precipitation records from Palolo (Fig. 3) (Giambelluca et al. 2011). Grand and Gaidos (2010) measured water table level in Ka‘au Crater for a total of five months (spanning 2003-

2004) and found fluctuations of 200 mm on a timescale of about 8 days. They also concluded that water-table level fluctuations were highly correlated with precipitation events, which are consistent with the results of this study. Overall, trends indicate that fairly small rainfall events are able to raise the water table level in the crater relatively quickly, whereas somewhat prolonged periods without rain lower the water table level.

2.2 Comparison of rainfall at contrasting mountain locations on Oʻahu

Precipitation is dynamic on the island of Oʻahu and changes dramatically from windward to leeward and coastal to mountain top locations. To better understand precipitation patterns at Kaʻau Crater, in the southeastern Koʻolau Mountains, two other mountain locations were chosen for comparison. To contrast locality in the Koʻolau Mountains, Poamoho was selected because it is located in the much wetter northern Koʻolau Mountains. As a comparison of rainfall patterns at windward versus leeward mountain ranges, Kaʻala in the Waianae Mountains was selected. In this exercise, the following question was posed:

Question 1: Is Kaʻau Crater representative of rainfall trends across mountaintop locations on Oʻahu?

Question 2: What are the relationships between El Niño Southern Oscillation (ENSO), the Pacific Decadal Oscillation (PDO) and mountaintop rainfall at windward vs. leeward locations?

Hypothesis 2: Kaʻau Crater and Poamoho will not reflect negative phases of ENSO and PDO as vividly as Mount Kaʻala due to their windward locations.

Kaʻau Crater is (Fig. 2) is approximately 450 m in diameter, with the crater floor located at an elevation of 460 m (Grand and Gaidos 2010). The extinct Kaʻau volcanic crater (21° 20’ 00” N, 157° 46’ 30” W) is a wetland today, where the dynamic water table is close to, or slightly above the surface of the soil (measured to be on an average 223 mm below the maximum measured water table position) and is maintained by high annual precipitation in addition to poor drainage, thus giving the crater a dynamic hydrology (Grand and Gaidos 2010). The crater is thought to have formed from post-shield rejuvenation stage volcanic activity that occurred about 1 million years ago (Macdonald et al. 1983). Kaʻau Crater is part of the Honolulu Volcanic Series, an assemblage of under-saturated volcanic rock, composed of melilite nephelinite magma. The underlying units of the Koʻolau shield volcano have a high hydraulic conductivity (~20 m hr^{-1}) (Oki et al. 1999); however, the crater itself was initially occupied by a lava lake that created a relatively impermeable floor (Macdonald et al. 1983). The lava lake bed, subsequent sedimentation, and accompanying low hydraulic conductivity created conditions for the formation of a swamp ecosystem that may possibly have been present, although perhaps intermittently, for tens or even hundreds of thousands of years. Surface drainage is assumed to occur through a single breach in the crater wall (Grand and Gaidos 2010). The rainfall station used for this long-term cross-location comparison is the Palolo VY BWS (718) station, located at 21° 19' 18.6" N, 157° 46' 18.1" W at an elevation of 301.8 m (Giambelluca et al. 2011). Monthly rainfall averages from 1920 to 2007 at the Palolo station show the wet winter and dry summer trends typical in Hawaiʻi (Fig. 3). On average, March received the greatest rainfall amount, 12.94 mm, and September received the least rainfall, 7.94 mm (Fig. 3). The average total wet season rainfall per year at the Palolo station is 1495 mm (Giambelluca et al. 2011).

Sediment accumulation environments suitable for stratigraphic paleoscience studies including pollen in mountaintop locations, relatively unaffected by humans, are somewhat rare. Poamoho (21° 30' N, 157° 54' W) is located in the northern Koʻolau Mountains, just northwest of Kaneohe near the Helemano Military Reservation (Fig. 2). The Koʻolau Mountains are the remains of the Koʻolau volcano, which began forming after the Waianae volcano (Macdonald et al. 1983). Two ponds with surrounding swampy vegetation rest in Poamoho at an elevation of 683 m within the Ewa Forest Reserve. Native vegetation such as *Metrosideros polymorpha* (Ohiʻa lehua); *Acacia koa*; and *Dicranopteris linearis* (uluhe ferns); along with invasive species such as *Psidium cattleianum* (waiawi, strawberry guava) surround the ponds. The Poamoho ponds are the headwaters of the Poamoho watershed, which feeds the Wahiawa watershed. The nearest rainfall station is the Poamoho No. 1 (883.12) station located at 21° 32' 0.3" N, 157° 56' 12.1" W at an elevation of 597.6 m (Giambelluca et al. 2011). The average total wet season rainfall per year at Poamoho from 1920-1997 is 2045.6 mm (Giambelluca et al. 2011).

Mount Kaʻala (Kaʻala) (21° 30' N, 158° 5' 59" W) is the tallest peak on the island of Oʻahu, at an elevation of 1,226 m above sea level (Fig. 2). Kaʻala is located in the northern Waianae Mountains, which are the eroded remains of an ancient shield volcano, which formed nearly 4 million years ago and went extinct much earlier than the Koʻolau volcano (Macdonald et al. 1983). The Kaʻala area is part of the Hawaiʻi Natural Area Reserves System and is home to 208 native plant taxa, 69 of which are rare (Corn 1992). Vegetation on Kaʻala includes native species such as *Metrosideros polymorpha* (Ohiʻa lehua); *Dicranopteris linearis* (uluhe ferns); and *Sadleria cyatheoides* (ʻamaʻu). Non-native species present include *Clidemia hirta* (clidemia*); Psidium cattleianum* (waiawi, strawberry guava); *Sphagnum palustre*; and *Pennisetum clandestinum* (*kikuyu grass*) (Wagner et al. 1990). The Mount Kaʻala (884) rain station sits at an elevation of 1224.1 m and is located at 21° 30' 28" N, 158° 8' 33" W. The average wet season rainfall total at the Kaʻala station from 1920-1997 is 1125.3 mm (Giambelluca et al. 2011). This study's analyses of weather patterns from Kaʻala show distinctive patterns from the sites in the Koʻolau Mountains. Kaʻala is located leeward of the Koʻolau Mountains, receiving different orographic rainfall trends than Kaʻau Crater and Poamoho pond.

Rainfall at Kaʻau Crater (Palolo station), Poamoho and Kaʻala was evaluated in terms of yearly totals, relationship with ENSO and relationship with the PDO from the year 1920 until 2007. The yearly rainfall averages for the 87 year period are: Palolo, 3266.3 mm; Poamoho, 4571.8 mm; and Kaʻala, 1921.1 mm. Poamoho consistently received 33% more annual rainfall than Palolo, while Ka'ala consistently received less rainfall averaging 48% lower than Palolo (Fig. 4). Poamoho also received the greatest amount of wet season rainfall, 550.6 mm per wet season more than Palolo and 920.3 mm more than Kaʻala. Poamoho is more than 200 m higher in elevation than Palolo, and orographic effects likely deliver more constant and intense rainfall at Poamoho. As Poamoho is in the northern Koʻolau Mountains, and winds tends to blow from the northeast, the delivery of moisture to the northeastern portion of Oʻahu may be greater than the southeastern area (Lau and Mink

2007). Incoming frontal systems and other westerly disturbances interact with the complex topography to produce the complex rainfall patterns in this region. Poamoho and Palolo both received more rainfall than Ka'ala throughout most years, which can be explained simply by the windward and leeward locations. Windward areas receive the most rainfall due to orographic lifting and leeward areas tend to be dry because air sinks and warms on the leeward side of mountains, suppressing the development of rain showers, a phenomenon known as the rain shadow (Chu and Chen 2005).

The El Niño3.4 index tends to have an inverse relationship with rainfall at all three sites, so that when ENSO is in a negative phase, the sites are generally positive in rainfall (Fig. 5, Fig. 6), although rainfall does fall in and out of phase with ENSO throughout all three records. From 1920 to about 1935 for example, when PDO is in a positive phase, the rainfall anomaly at Palolo is below average, Poamoho shows positive anomalies followed by negative rainfall anomalies and Ka'ala exhibits strong negative rainfall anomalies (Fig. 5, Fig. 6). A clearer inverse relationship between PDO and rainfall is observed at Palolo and Poamoho than Ka'ala especially between 1945 and 1975, with more variability from 1975-2007 (Fig. 5). Overall, no concrete relationships are apparent because all three sites tend to fall in and out of phase with both ENSO and PDO throughout the past ninety years. Ka'ala is the only site with a significant relationship with PDO (p=0.009) (Fig. 7). Ka'ala is the tallest area on O'ahu, therefore this area may be more affected by PDO due to elevation. Poamoho appears to be wet regardless of the PDO phase.

This comparison of rainfall across mountain-top locations reveals some valuable insights. All three locations follow the relative wet season and dry season pattern of Hawaiian rainfall. Poamoho receives the most rainfall regardless of season, due to its elevation and windward location. Ka'ala is nearly as wet at Palolo during the wet season, but is much drier than Palolo and Poamoho during the dry season because of its leeward location. Palolo receives moderate rainfall compared to the extreme wet and dry conditions of Poamoho and Ka'ala, respectively. The linear regression reveals insignificant results between rainfall and PDO for both Palolo and Poamoho; however, Palolo does have more apparent positive relationship with PDO than Poamoho (Fig. 7). Both sites appear to be equally responsive to El Niño (Fig. 6 b, Fig. 6 d). It may be inferred, that Palolo is more affected by long-term phase-changes of PDO than Poamoho. Furthermore, more confidence may be put in the vegetation reconstruction of Ka‘au Crater as in indicator of large-scale atmospheric change. Ka‘au Crater appears to be responsive to atmospheric modes and also wet enough to allow consistent existence of the swamp and accumulation of sediments

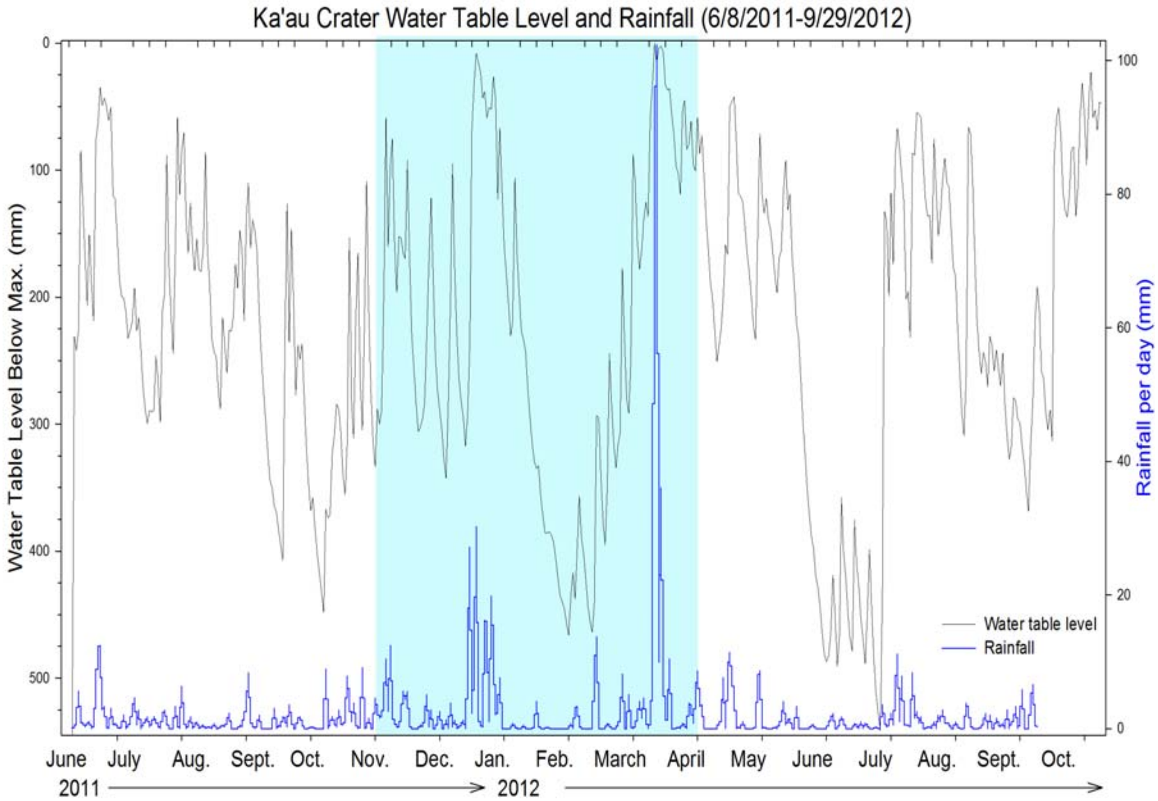

Fig. 1. The water table level in Ka'au Crater was recorded from June 8, 2011 to September 29, 2012. Rainfall values are from the Hawai'i Archived Hydronet Data, HI-25 Palolo FS PFSH1 station.

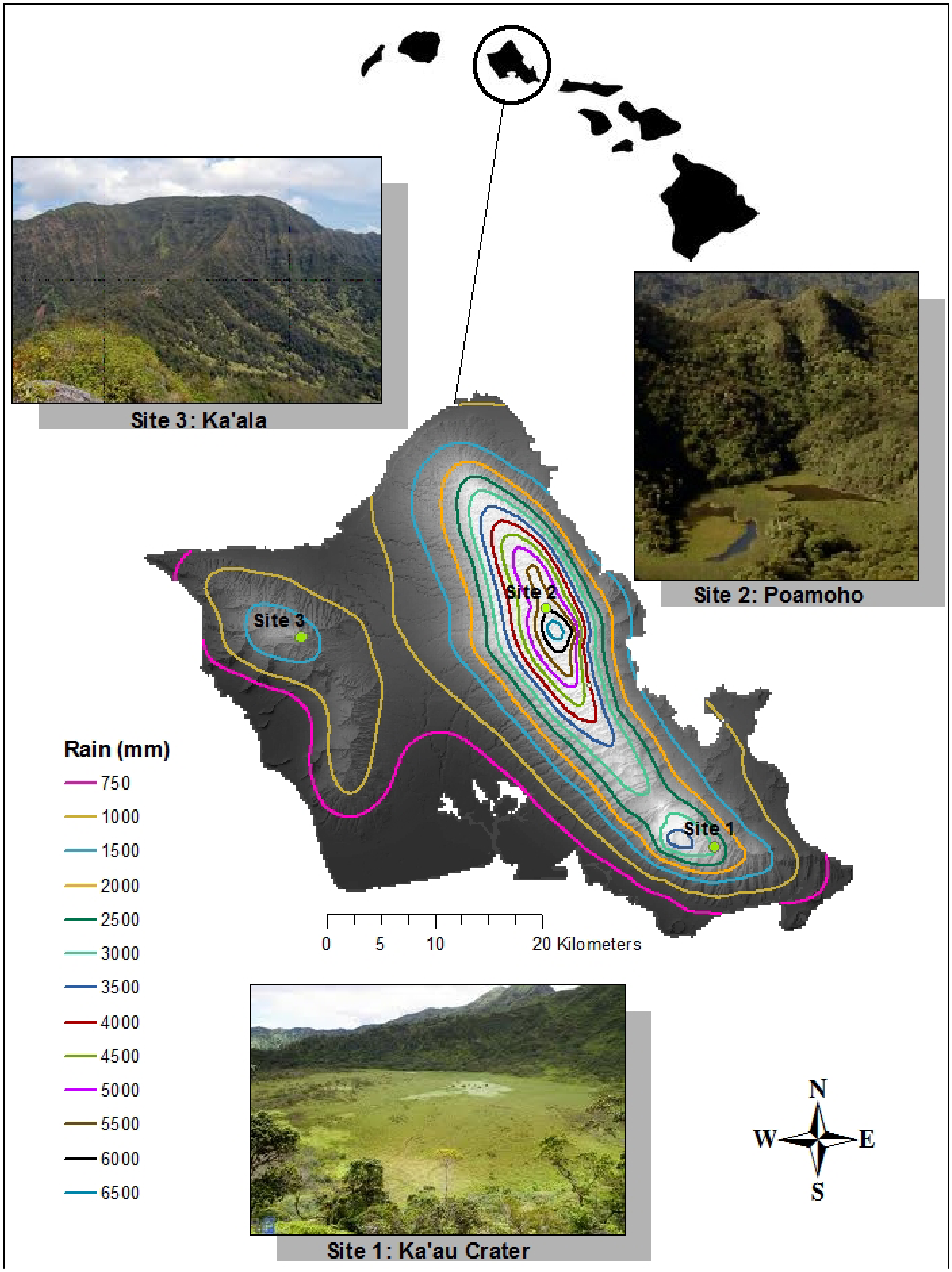

Fig. 2. Mountain locations of consideration for this study on O'ahu, Hawai'i. Ka'au Crater is located in the southern Ko'olau Mountains at an elevation of 460 m. Poamoho is located in the northern Ko'olau Mountains at an elevation of 597.6 m, and Ka'ala is located in the northern Waianae Mountains on the leeward side of O'ahu. Isohyets are presented in millimeters (Giambelluca et al. 2011).

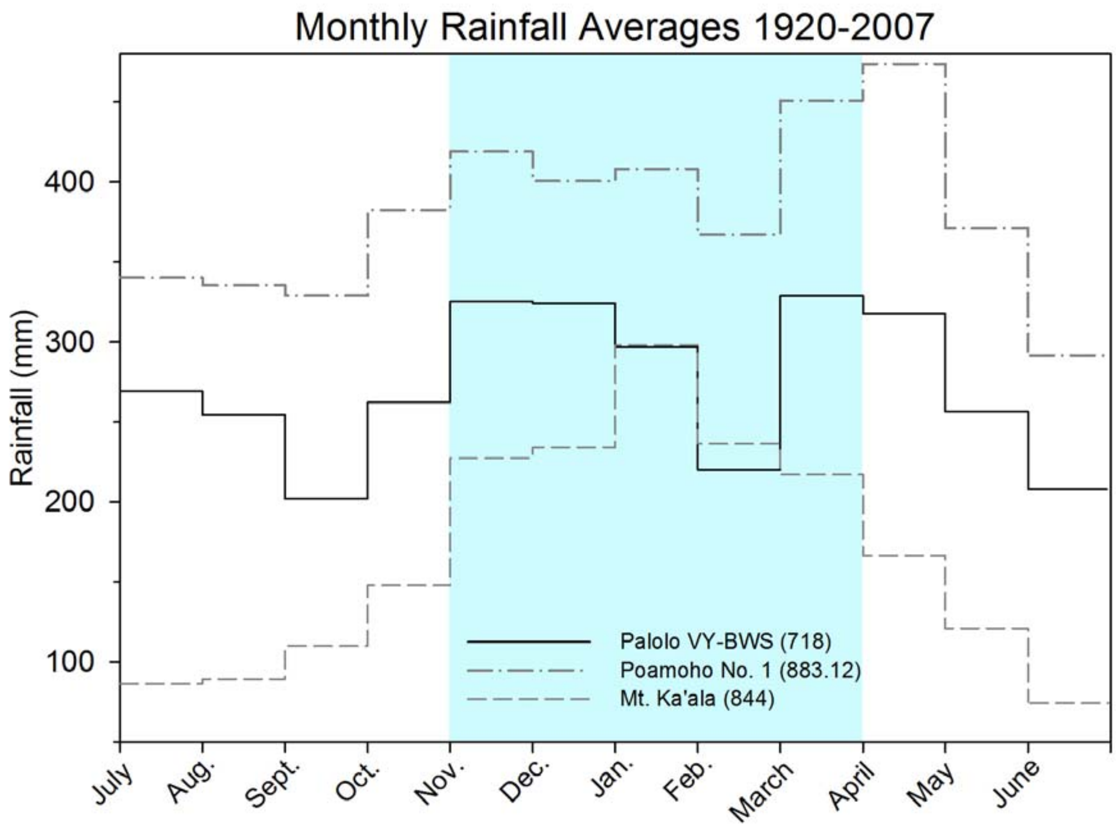

Fig. 3. Average monthly rainfall values for Palolo, Poamoho and Mt. Ka'ala from Giambelluca et al. (2011).
*The blue shading indicates the winter wet season from November through March (Chu and Chen 2005).

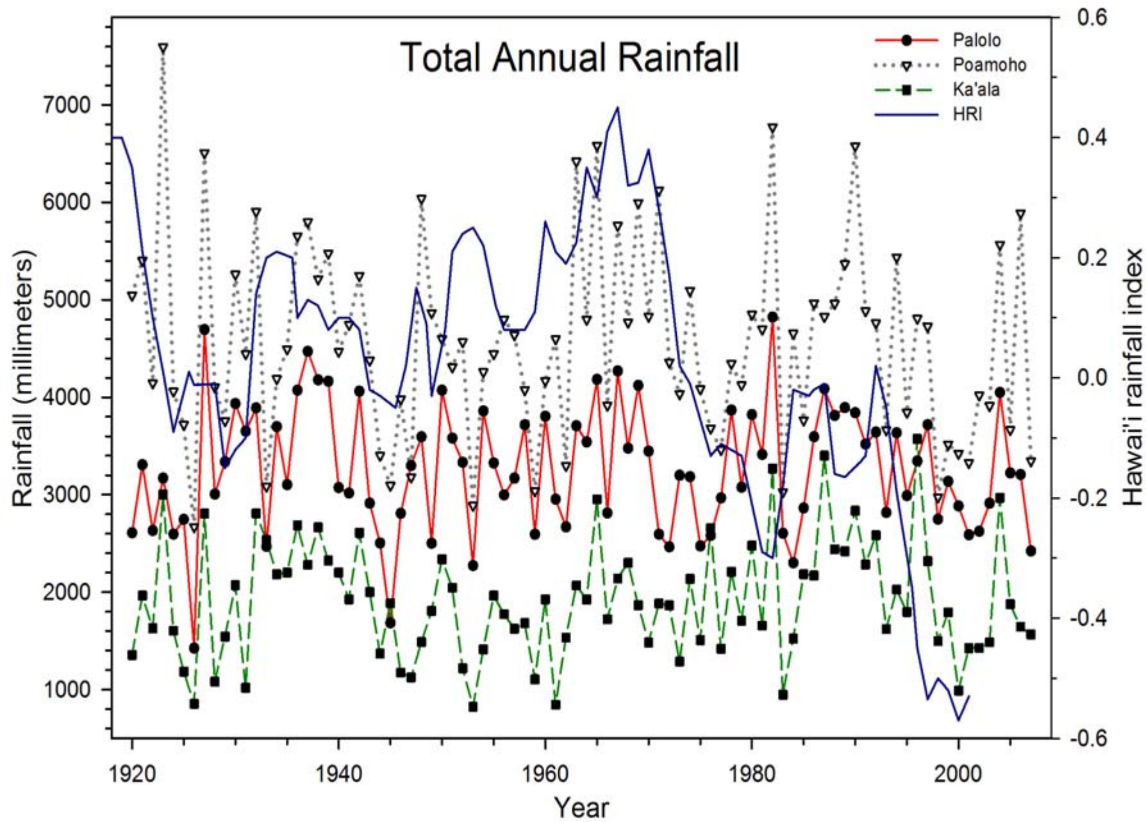

Fig. 4. Average annual rainfall values for the Palolo, Poamoho and Ka'ala rain stations from Giambelluca et al. (2011). The Hawai'i rainfall index (HRI), developed by Meisner (1976), was created using data from 27 stations across Kaua'i, O'ahu and Hawai'i Island and represents rainfall variations over different climate regions of the Hawaiian Islands (Chu and Chen 2005).

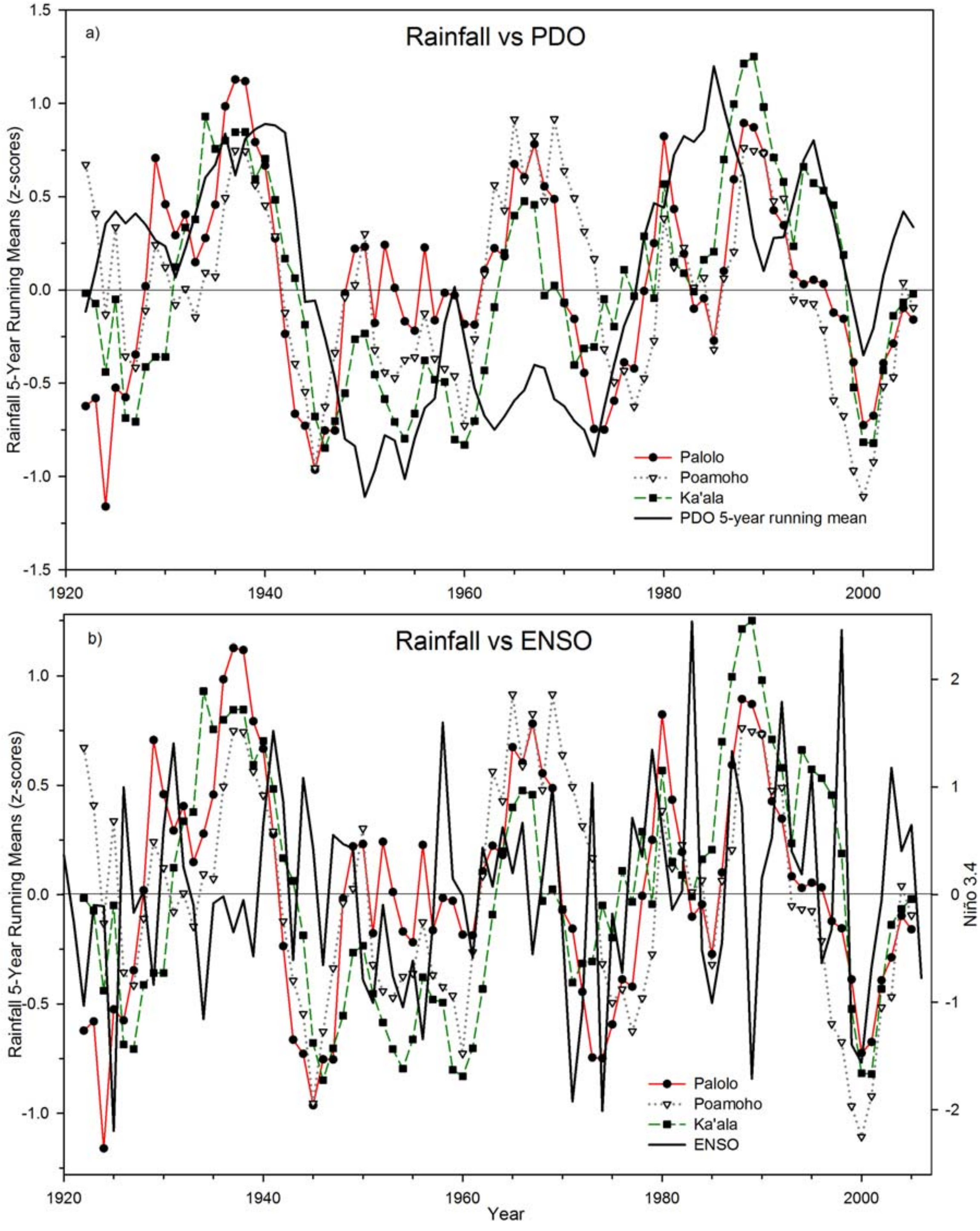

Fig. 5. Five-year running means of rainfall z-scores for Palolo, Poamoho and Ka'ala (Giambelluca et al. 2011) compared to the five-year running mean of the PDO (a) and to El Niño Southern Oscillation (Niño3.4 index) (b). The Niño3.4 index is used because it is more representative of ENSO than other indices (Chu and Chen 2005). In the Niño-3.4 index, El Niño (La Niña) occurs if a 5-month running mean of SST anomalies in the Niño-3.4 region (5° N-5° S, 120°-170° W) exceeds 0.4°C (-0.4°C) for six consecutive months or more (Trenberth 1997).

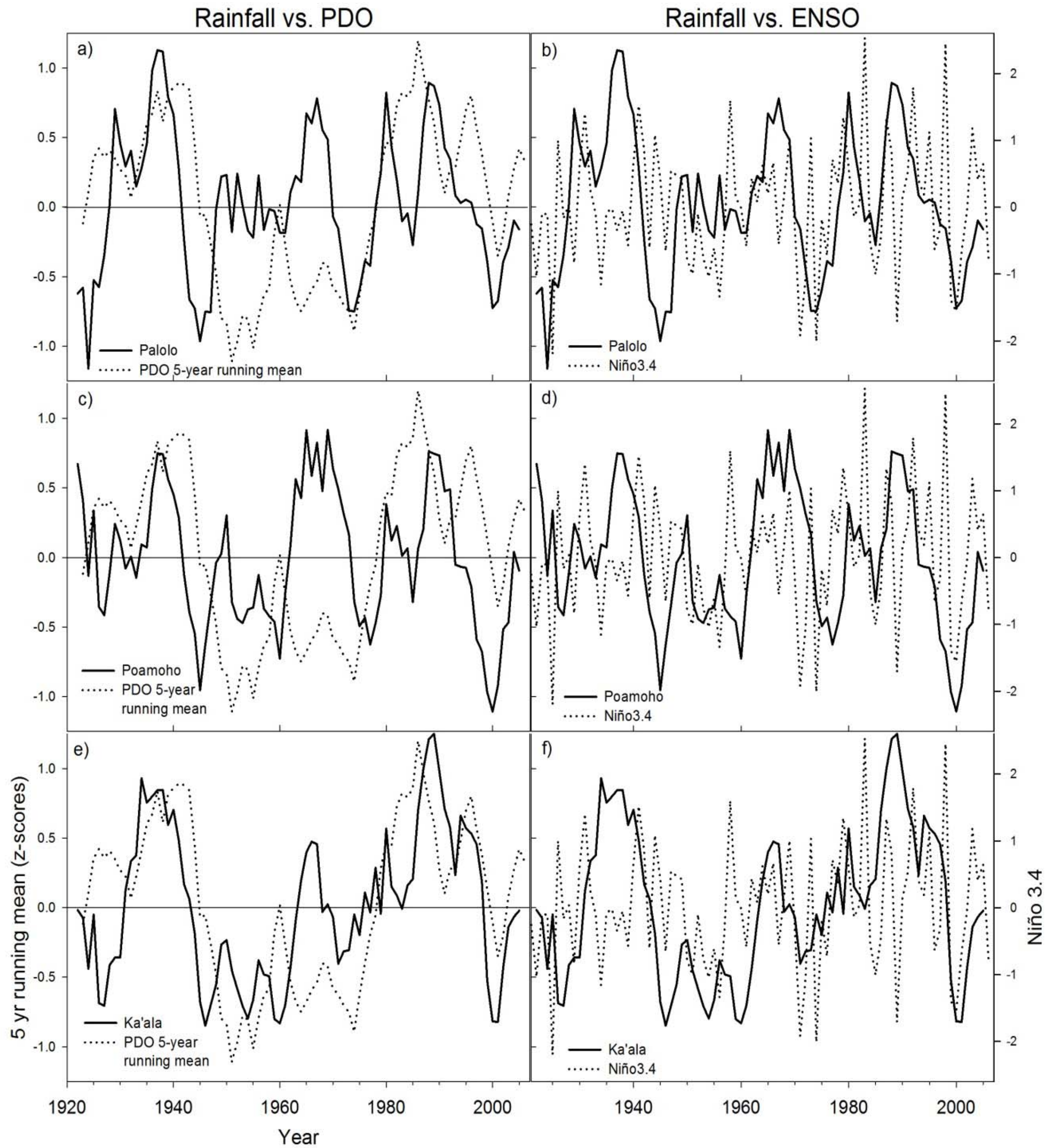

Fig. 6. Individual plots of five-year running means for Palolo, Poamoho and Ka‘ala rainfall (Giambelluca et al. 2011) vs. the five-year running mean of PDO (a, c, e) and ENSO (Niño3.4 Index) (b, d, f).

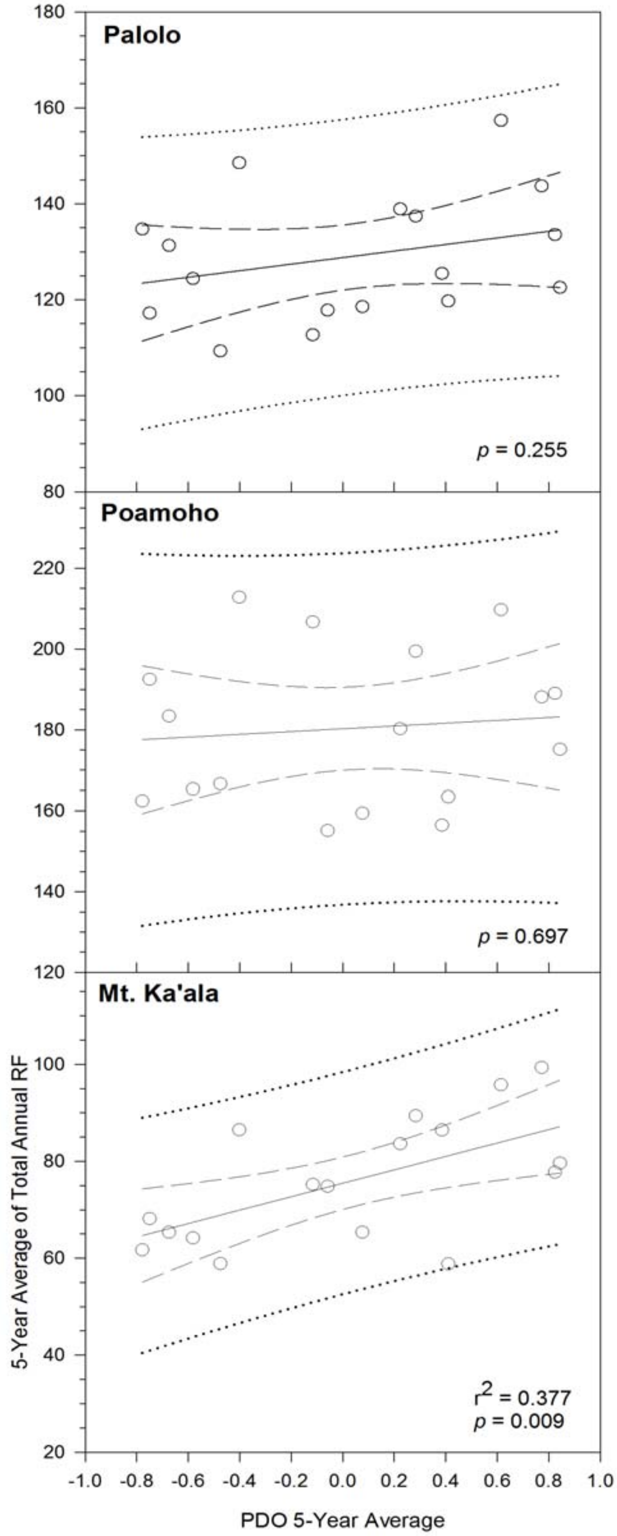

Fig. 7. Total annual rainfall summed in five-year increments for each site (rainfall data from Giambelluca et al. 2011) regressed with the five-year means of PDO for the same time periods. The first period is from 1920-1924 and the last is 2000-2004.

2.3 Literature Cited

Chu, P.-S., and Chen, H. 2005. Interannual and Interdecadal Rainfall Variations in the Hawaiian Islands. *Journal of Climate* 18, 4796-4813.

Corn, Carolyn A. *Kaʻala bog plant guide: Kaʻala Natural Area Reserve : Mt. Kaʻala, Oʻahu*. Oʻahu, Hawaiʻi: Dept. of Land and Natural Resources, Division of Forestry and Wildlife, 1992. Print.

Giambelluca, T.W., Chen, Q., Frazier, A.G., Price, J.P., Chen, Y.-L, Chu, P.-S., Eischeid, J., and Delparte, D. (2011). The Rainfall Atlas of Hawaiʻi.

Grand, M., and Gaidos, E. 2010. Methane Emission from a Tropical Wetland in Kaʻau Crater, Oʻahu, Hawaiʻi. *Pacific Science* 64(1), 57-72.

"Hawaiʻi Archived Hydronet Data." *National Weather Service Pacific Region Headquarters*. N.p., n.d. Web. 30 Sept. 2012. <http://www.prh.noaa.gov/hnl/hydro/hydronet/hydronet-data.php>.

Lau, S.L., and Mink, J.F. *Hydrology of the Hawaiian Islands*. Honolulu: University of Hawaiʻi Press, 2006. Print.

Macdonald, Gordon A., Townsend Abbott, Agatin, and Peterson, Frank, L. Volcanoes in the Sea: the geology of Hawaiʻi second edition. Honolulu: University of Hawaiʻi Press, 1983. Print.

Oki, D.S., Gingerich, S.B., and Whitehead, R.L. 1999. Ground Water Atlas of the United States: Alaska, Hawaiʻi, Puerto Rico and the U.S. Virgin Islands, USGS.

Wagner, Warren Lambert, Herbst, Derral R., and Sohmer, S.H. *Manual of the flowering plants of Hawaiʻi*. Honolulu: University of Hawaiʻi Press: 1990. Print.

CHAPTER 3. VEGETATION, TEMPERATURE AND PRECIPITATION RECONSTRUCTIONS FOR KAʻAU CRATER THROUGH THE HOLOCENE

3.1 INTRODUCTION

Palynology is one of the most widely used research tools in Quaternary Studies (Edwards 1983). Data derived from the study of fossil pollen and other environmental proxies can indicate the response of natural vegetation to human impacts through time, as well as to climatic and environmental change (Prentice 1988). In Hawaiʻi, Selling (1946, 1947, and 1948) conducted palynological surveys on the islands of Maui, Kauaʻi and Molokaʻi, which included investigations using tropical peats, and documented patterns of marked change in some of the first complete pollen diagrams from the tropics (Burney et al. 1995). Selling (1948) studied "raised bogs and soligeneous swamps" on Kauaʻi, Molokaʻi, Maui, and Hawaiʻi between elevations of 1200 m and 1765 m and found initial stage conditions for bogs in the Koʻolau Range, at the head of the Kaipaupau and Kawainui gorges on Oʻahu. Selling (1948) recognized three main periods in his study of paleo vegetation, to which dates were not assigned, as advanced dating methods were not yet available. Drier vegetation types were recorded at near surface levels of Selling's sediment cores, followed by an expanding rainforest, and lastly rainforest replaced by drier vegetation types in the deepest core sections. Although Selling's early investigations could provide no absolute dates to his observed vegetation changes, this early work showed that plant communities have been dynamic in Hawaiʻi. Since Selling, other paleoecological studies have been carried out in Hawaiian lowlands (Athens et al. 1992; Athens et al. 1996; Athens 1997; Crausbay 2011; Pau et al. 2012), as well as at higher elevation sites (Burney et al. 1995; Hotchkiss and Juvik 1999), analyzing vegetation dynamics after the last glacial maximum and during the Holocene.

Organic soils are formed by plant debris and are often found in wetland ecosystems because soil decomposition is depressed and organic matter stabilization is promoted in wet settings (Richardson and Vepraskas 2001). Histosols are the organic-rich order of peat and muck soils that generally favor the balance of organic matter accumulation over decomposition. Histosols occur most commonly in high-latitude boreal and subarctic regions, but also form in the tropics in areas with constrained drainage such as wetlands (Sumner 2000). The total area of histosols worldwide is estimated at 3.25-3.75 million square kilometers, with one-tenth of the total located in the tropics (Driessen 2001).

Tropical peat can be found in mountain elevations and low-lying areas where substantial rainfall and topography provide appropriate conditions for poor drainage, permanent water logging, and substrate acidification (Jauhiainen et al. 2005). Peat is a highly variable substance composed partially of decomposed remains of plants with over 65% organic matter and less than 25-30% inorganic content (Charman 2001). Tropical peatlands are of interest to scientists and global leaders owing to their distinct biodiversity, their large existing pool of organic carbon, and the potential sensitivity of this carbon to decomposition and flux of methane and carbon dioxide to the atmosphere owing to climate change and rapidly increasing human populations causing land degradation. Highland and coastal tropical peatlands are poorly studied relative to their global counterparts.

From the point of view of carbon accumulation in tropical histosols, Yu et al. (2010) documented from a handful of available records rapid peat carbon accumulation rates in the tropics about 8000–4000 cal yr BP, asserting that carbon accumulation dynamics in tropical peatlands (mainly in Southeast Asia) were likely affected by summer monsoon intensity, sea level change and El Niño intensity. The abundance of volcanic islands in the tropical Pacific and the high elevation mountainous locations they boast offer numerous opportunities for paleoclimate reconstructions. Hotchkiss and Juvik (1999) analyzed a soil core from Ka‘au Crater, O‘ahu dating from approximately 25,800 cal yr BP to 8120 cal yr BP. Their sediment core captured substantial and sensitive vegetation change through the last glacial maximum and into the early Holocene. They documented lower precipitation in Ka‘au Crater during the late glacial period and last glacial maximum; however, their record did not span the Holocene. The age-depth model in Hotchkiss and Juvik (1999) was constructed using five ^{14}C dates, ranging 8120-25,860 cal yr BP between depths 50-310 cm, although a reversal occurred between the two oldest dates, therefore a linear interpolation of possible chronologies was constructed.

3.1.1 Objectives

It has been recognized that paleoclimate records from the tropics are lagging compared to evidence from the high-latitudes (Cane 1998). The tropics, covering half of the Earth's surface, are capable of producing global interannual climate variability such as the El Niño-Southern Oscillation (ENSO), which is the largest single source of global interannual climate variability (Chiang 2009). Terrestrial paleoclimate records for Oʻahu have contributed significantly to the paleoclimate literature (Athens and Ward 1993; Burney et al. 1995; Hotchkiss and Juvik 1999), although much remains to be learned about the most recent past of the Holocene, in terms of precipitation and climate patterns affecting mountain locations. Water availability today and in the near future has become a public concern as growing demand puts more pressure on Hawai'i aquifers and the effects of climate change continue to materialize. Therefore, the goals of this research were to provide a comprehensive Holocene record of vegetation change over time from which precipitation and temperature may be deduced, and to present vegetation and drought data that may be utilized by scientists and planners not only islands-wide but throughout the Pacific to bridge gaps in and between paleo-data in Hawai'i and the tropics. The overarching objective of this research project was to expand climate records from Oʻahu for the Holocene in terms of the following questions concerning vegetation, mountain locations, and multidecadal atmospheric patterns:

Question 3: What were vegetation community composition dynamics in and near Kaʻau Crater, Oʻahu, a mountain wetland, during the Holocene?

> **Hypothesis 3:** A wide variety of plants existed in high elevations during the past 10,000 years including those best suited for precipitation ranges of dry (i.e. Chenopodiaceae), dry-mesic (i.e. Rubiaceae), mesic-wet (i.e. Urticaceae), wet (i.e. Rutaceae) and dry-wet (i.e. Myrsinaceae). Uchikawa et al (2010) recorded an expansion of C_4 plants from 10,000-6000 cal yr BP suggesting a reduction in water availability; therefore, it follows that vegetation best-suited for dry, dry-mesic, and mesic were more abundant during this time-span (10,000-6,000 cal yr BP) than mesic-to-wet and wet-tolerant plants.

Question 4: Have there been long periods with multiple extensive droughts on the island of Oʻahu during the Holocene?

Hypothesis 4: Pollen from abundant dry-tolerant plants, such as Rubiaceae (tree/shrub species), Santalaceae (sandalwood), and Polypodiaceae (terrestrial and epiphytic ferns) have increased and sustained higher abundances for periods of a few hundred years or longer.

3.1.2 Site Description

Kaʻau Crater, located in the southeastern portion of the Koʻolau Mountains on the island of Oʻahu at an elevation of 460 m, receives an annual average of 3302 mm of precipitation (Fig. 2) (Giambelluca et al. 2011). The most recent vegetation survey was conducted by Kennedy (1975) who described five major vegetation communities in the crater. The vegetation assemblage is a mixture of native and invasive species such as *Dianella sandwicensis* (Liliaceae, uki), a native sedge; *Metrosideros polymorpha (*Myrtaceae) (`ōhi`a lehua), a native tree; *Cordyline terminalis* (tī leaf), an ornamental plant; and *Psidium cattleianum*, (waiawi, strawberry guava), an invasive tree (Kennedy 1975). The native sedge *Cladium mariscus* (Cyperaceae*)* [identified as *Cladium leptostachym* (uki) by Kennedy (1975) and *Cladium jamacense* by Elliot and Hall (1977)], which comprises the largest group, is a non-woody, grass-like plant, and is defined by Gagné and Cuddihy (1990) and Wagner et al. (1990) as living in the dry-wet precipitation range. The second major vegetation type is a floristically diverse open scrub that includes dwarfed *Metrosideros polymorpha*, classified in the dry-wet precipitation range as well (Grand and Gaidos 2010). A dendrochronological study was done in Kaʻau Crater in 2012 which included several measurements of radiocarbon content of tree wood, and suggested `ōhi`a is a more recent inhabitant of the crater floor [samples: UBA-18782, $F^{14}C$: 1.2146; UBA-18783, $F^{14}C$: 1.2299; UBA-18784, $F^{14}C$: 1.2848; UBA-18785, $F^{14}C$: 1.2378; UBA-18786, $F^{14}C$: 1.1272 (David Beilman, unpublished data)].

The third vegetation class contains the non-native *Cordyline terminalis* (Agavaceae) (tī) which does not have a listed precipitation range in Gagné and Cuddihy (1990) or Wagner et al. (1990) but commonly exists in moist to wet habitat (Sohmer and Gustafson 1987). The non-native *Commelina diffusa* (Commenlinaceae) (honohono) also occurs sparsely in this group along with the indigenous bulrush *Shoenoplectus lacustris* (Cyperaceae) (honohono), which again is in the dry-wet precipitation range. Kennedy's fifth group lists a dense forest of the invasive *Psidium cattleianum* (Myrtaceae) (strawberry guava) which occupies the crater floor in the vicinity of the outlet stream and the inner slopes of the crater wall and is also in the dry-wet precipitation range defined by Gagne´ and Cuddihy (1990) and Wagner et al. (1990) (Grand and Gaidos 2010).

In Hawai'i, rainfall plays the dominant role in determining the rate of soil formation as well as the characteristics of the soil produced; the great variations in annual rainfall occurring in short distances produce correspondingly great differences in soils (Ripperton and Hosaka 1942; Townsend et al. 1995). Ka'au Crater soils consist of a mucky peat, characteristic of bogs and mountain tops which makes up the majority of crater floor (Foote 1972). The mucky peat soil in the crater has a layer that impedes the downward movement of water therefore generating a slow infiltration rate (Foote 1972). The soil on the rough mountainous land surrounding the crater floor is silty clay loam from alluvium and colluvium parent material which also has a very slow infiltration rate (high runoff potential) when thoroughly wet (Foote 1972). A dam and reservoir were constructed in Ka'au Crater in the late 1800s (Elliot and Hall 1977) that failed at some point in the early 1900s, apparently resulting in erosion of a significant amount of soil and sediment in some parts of the crater (Hotchkiss and Juvik 1999).

Hawai'i is situated in the trade-wind zone and experiences relatively small day-to-day variations in weather (Garza et al. 2012). On the southern coast of O'ahu, as is the case for most places in Hawai'i, northeasterly winds blow from 85 to 95% of the time in the summer, and from 50% to 80% of the time in the winter (Sanderson 1993). As Ka'au Crater lays just south of the Ko'olau Mountain ridge, the trade winds and orographic uplift play a dominant role in the precipitation received.

3.2 METHODS

3.2.1 Sediment coring

In order to explore the historical vegetation composition in Ka‘au Crater, a sediment core was raised from near the center of the crater in 2009. One continuous soil core 450 cm in length was extracted using a rotating-sleeve side-cut ‘Russian’ corer with an inside core diameter of 5 cm. The core was taken 50 cm at a time, then packaged in plastic film and aluminum foil and stored frozen within 6 hours. After freezing, all sediment core sections were cut into one-centimeter slices with a cleaned stainless steel blade on a band saw and stored frozen in individual water-tight plastic bags.

3.2.2 Radiocarbon dates and chronology

Fourteen 1-2 cm^{-3} bulk sediment and three fine-fraction (<150 μm) samples were measured for ^{14}C content following standard ABA pretreatment at the ^{14}CHRONO Centre at Queens University Belfast. The program Calib Rev 6.1.0 was used to convert radiocarbon ages to calendar years BP using the IntCal09 calibration curve (Reimer et al. 2010). A chronology for the sediment profile was created in the Tilia program by fitting a spline B-curve through the calibrated radiocarbon (^{14}C) bulk sediment dates (Grimm 1991). Three levels in the core were processed for both bulk dates as well as isolation of the sediment fine-fraction less than 150 microns; bulk and fine-fraction dates were fairly similar for the samples (within 113-478 calendar years); lending some support to the reliability of bulk sediment ages. An age-depth model for the sediment profile was created in the Tilia program by fitting a spline B-curve through the calibrated radiocarbon (^{14}C) bulk sediment dates.

3.2.3 Bulk density and organic matter assays

Bulk density is defined as the mass of a unit volume of dry soil, or the ratio of the mass to the bulk volume of soil particles plus pore spaces in the sample (Brady and Weil 2002). The bulk density depends on many soil conditions such as compaction, puddling, management and cultivation (Chesworth 2008). Bulk density was calculated on a known volume of fresh soil, 0.67-2.34 cm^{-3}, by drying the soil then dividing the dry weight by the initial sample volume to arrive at the bulk density value in g cm^{-3} (Schaetzl and Anderson

2005). Ash-free bulk density, a proxy for degree of peat decomposition and thus moisture conditions, was calculated from measurements of sample volume, dry weight and organic contents. The ash weight was subtracted from the dry weight then divided by the sample volume (Yu et al. 2003).

The loss on ignition (LOI) process is frequently used to estimate the organic content of various sediments (Wang et al. 2011). Determination of weight percent organic matter in sediments by means of LOI is based on sequential heating of the samples in a muffle furnace and was carried out using the methods in Dean (1974) and a modified version of Heiri et al. (2001). The LOI of Ka‘au Crater sediment was calculated using the following equation: $LOI_{550} = ((DW_{95}–DW_{550})/DW_{95})*100$, where LOI_{550} represents LOI at 550°C (as a percentage), DW_{95} represents the dry weight of the sample before combustion and DW_{550} the dry weight of the sample after heating to 550°C (both in g); the weight loss is proportional to the amount of organic matter contained in the sample (Heiri et al. 2001). The LOI process was carried out on every-other sliced level of the Ka‘au Crater sediment core from sample 2 to sample 450. The sediment accumulation rate was found by dividing the difference in depth between radiocarbon dated samples and then dividing by the number of years between each interval. The organic matter accumulation rate was calculated by summing ash-free bulk density values between radiocarbon dated samples, multiplying by two (to account for odd-numbered samples not processed), then dividing by the number of years between each interval. Lastly, values were multiplied by 10,000 to convert from centimeters squared to meters squared.

3.2.4 Stable isotopes of carbon and nitrogen

Stable isotope values of carbon and nitrogen in bulk sediment were measured by EA-IRMS at the Isotope Biogeochemistry Laboratory at the University of Hawai‘i, School of Ocean, Earth and Science Technology. Approximately 1 cm^{-3} sediment subsamples from 55 levels of the core were homogenized to <250 μm and 2-8 mg subsamples were loaded into Sn capsules depending on their organic matter content as measured by LOI.

3.2.5 Laboratory pollen preparation

When preparing samples for pollen counting, the objective is to concentrate pollen, spores and other microfossils in the sediment by removing extraneous matter, and to render them as visible as possible by staining them (Faegri and Iverson 1989). Twenty levels of the 450 cm sediment core were selected, based on the radiocarbon dates and each sub-sampled for 1 cm^{-3} volume of material. Pollen was isolated from other soil constituents using a modified version of the laboratory technique of Faegri and Iverson (1989): soil samples were treated with a 10% hydrochloric acid solution to remove carbonates; a tablet containing 20,848 spores of *Lycopodium* (from Lund University, batch 1031 (2011)) was added to quantify concentration and accumulation rates during pollen counting; short-chain organic acids were removed by the addition of a 10% potassium hydroxide solution; hydrofluoric acid (50%) was added to dissolve silicates; and cellulose in the sediment was removed by the addition of an acetolysis mixture of nine parts acetic anhydride to one part sulfuric acid. Sediment samples were rinsed with 18.3 mega-ohm-cm deionized water, centrifuged at 2.5 rpm for four minutes and decanted 1-8 times between treatments. Following the chemical treatments, samples were sieved with a 300-micron screen to remove large, non-pollen particles. Safranin cell wall stain was added for easier viewing in the pollen counting stage. Pollen was lastly mounted with silica oil, 2000 centistokes, onto microscope slides and covered with a slide cover for viewing (Faegri and Inverson 1989).

3.2.6 Pollen stratigraphy

Pollen percentages were based on a pollen sum of at least 200 grains of terrestrial pollen and spores. This number was chosen based on the fact that fossil pollen concentrations in Hawaiian sediment cores are typically too low to achieve higher minimum pollen sums (Pau et al. 2012; Athens et al. 1992; Athens et al. 1996). A Zeiss Scope.A1 was used at a magnification of 400× to view all pollen and spores. *Lycopodium* (batch 103) spores were summed and recorded for each level to quantify pollen concentration and accumulation rates. Pollen grains and spores were identified to the lowest taxonomic level possible using a reference collection (Stephanie Pau, personal communication) along with photos and descriptions in Selling (1946, 1947, and 1948). The program Tilia was used to quantify pollen abundances, sums, percentages and influx (Grimm 1991).

3.2.7 Temperature and precipitation reconstructions

Quantitative estimates of past climate were carried out using a transfer function which provides estimates of past climate based upon the relationship between modern climate and pollen deposition (MacDonald and Edwards 1991). Temperature and precipitation estimates, from Hotchkiss and Juvik (1999), were constructed using modern precipitation and elevation ranges of 83 plant species (Table 1). Hotchkiss and Juvik (1999) averaged the assigned climate values of each pollen type and weighted them by the pollen percentages to create each pollen type's climate estimate. Following Hotchkiss and Juvik (1999) pollen types were grouped into six precipitation range categories: dry (present ranges of all taxa included receive less than 1200 mm average annual precipitation), dry-to-mesic (<2500 mm), mesic (1200–2500 mm), mesic-to-wet (>1200 mm), wet (>2500 mm), and dry-to-wet (<1200 to >2500 mm), using range classes from Gagné and Cuddihy (1990) and Wagner et al. (1990). Hotchkiss and Juvik (1999) noted that the categorization of pollen types was particular; for example, species that are abundant in dry habitats but present infrequently in mesic and wet regions were classified as dry-to-wet.

The pollen abundance index (PAI) in Hotchkiss (1998), which was derived and tested on 102 surface samples from the island of Hawai'i to estimate past temperature and precipitation estimates, was utilized in the climatic reconstruction (Table 1). Pollen types were deemed rare if they were present in less than three surface samples and never more abundant than the value of the upper 95% confidence limit calculated by Hotchkiss and Juvik (1999). These rare types were eliminated from the PAI. Hotchkiss and Juvik (1999) also chose to exclude pollen types from the PAI if high pollen percentage values (>40% of the maximum value) ranged over 4°C or 2500 mm precipitation; in other words, if peak pollen percentages were not clearly defined with respect to climate. *Pritchardia* was excluded from the PAI because there is presently strong evidence that its current distribution is not an accurate indicator of precipitation; additionally, historic evidence indicates species in this genus once had a lowland leeward distribution and may only be restricted to higher elevation wet forests in the surface samples because of human-driven extirpation (Pau et al. 2012; Athens 1997; Burney et al. 2005)

3.3 RESULTS

3.3.1 Radiocarbon dates and chronology

The chronology of the core was based on ten radiocarbon dates of bulk sediment (Table 2, Fig. 8). The radiocarbon dates range from 1726 ^{14}C yr BP at 32 cm below the surface to 14,087 ^{14}C yr BP at 384 cm. Two reversals occur from sample HWI-KAA-163 to HWI-KAA-192 and again between HWI-KAA-384 and HWI-KAA-413. The last three dates in the deepest portion of the core are also inconsistent. Two of the fine fraction dates are very similar to the accompanying bulk sediment dates (within 113-117 calendar years), while the fine fraction date and bulk sediment dates of sample HWI-KAA-256 are in great disagreement (difference of 478 calendar years) (Table 2). The age-depth model shows a moderate accumulation rate between about 14000 and 6000 cal yr BP (Fig. 8). An increased sedimentation rate begins at approximately 6000 cal yr BP and continues until about 4450 cal yr BP (Fig. 8).

3.3.2 Bulk density and organic matter assays

The bulk density is rather consistent throughout the core with an average of 0.18 g/cm^3 (Fig. 9b). The bulk density ranges between 0.04-0.64‰, with an average of 0.17‰. Because clastic inorganic material can greatly increase peat bulk density values, calculating the ash-free bulk density can help remove the inorganic influence on density and reveal changes in organic matter density that may have been influenced by the degree of decomposition. The ash-free bulk density ranges between 0.03-0.16‰, with an average of 0.08‰. A period of greater ash-free bulk density persists from 6000 to about 5000 cal yr BP (Fig. 9c). Departures toward greater ash-free bulk density occur again between 3600 and 2000 cal yr BP (Fig. 9c). The sediment accumulation and organic matter accumulation rates show similar patterns, increasing relatively gradually at approximately 8000 cal yr BP and dramatically at about 5800 cal yr BP (Fig. 9f, Fig. 9g).

The LOI ranges from 10.75-93.56% with an average of 58.96% (Fig. 9a). From 9000 cal yr BP to about 7600 cal yr BP the percent LOI remains below 70% then increases to 90% shortly after 7600 cal yr BP (Fig. 9a). The percent LOI remains relatively consistent between 80-90% until about 5600 cal yr BP where a gradual yet significant decrease to 40% occurs (Fig. 9a). Two more increases in percent LOI occur at approximately 4550-4200 cal yr BP and 3500-3100 cal yr BP, both followed by decreasing percentages (Fig. 9a). Both the sediment accumulation and organic matter accumulation rates are relatively low for the majority of the record then dramatically increase around 5800 cal yr BP (Fig. 9 f, Fig. 9 g).

3.3.3 Stable isotopes of carbon and nitrogen

Stable carbon isotope ratios are a useful tool for understanding carbon and nitrogen cycling in peatlands, and provides a method for interpreting changes in temperature and moisture over long time periods (Jones et al. 2010). The amount of ^{13}C in the Kaʻau Crater sediment fluctuates between approximately -28.25‰ and -26.25‰ for the extent of the core (Fig. 9d). The ^{13}C is relatively stable from the bottom of the Kaʻau core, 9000 cal yr BP, until just after 8000 cal yr BP a gradual increase occurs followed by a great increase just after 7000 cal yr BP to -26.25‰ (Fig. 9d). Much variability occurs between 6100 and 4600 cal yr BP.

Any mechanism that leads to loss of N (volatilization, mineralization and leaching, plant uptake) will leave the heavier N isotope behind (Högberg 1997). The amount of ^{15}N shows substantial variation throughout the Kaʻau core with similar variability from 6100 to 4600 cal yr BP as the ^{13}C record. Lower ^{15}N values of 0.7-3.9‰ are recorded for the deepest portion of the Kaʻau core, 14,000-6200 cal yr BP, followed by a sharp increase beginning at about 6000 cal yr BP rising to approximately 5.7‰ at about 5600 cal yr BP (Fig. 9e). The ^{15}N amount stays relatively consistent throughout the remainder of the core. Histosols in the Everglades, Florida range in ^{15}N values from 3.86‰ in the topmost soil decreasing with depth to 2.98‰, which demonstrates the great variability of ^{15}N in histosols (Wright and Inglett 2009).

3.3.4 Pollen stratigraphy

Changes in terrestrial pollen spectra are shown for the past 7650 years (Fig. 10). Thirty-eight pollen types were identified in the Kaʻau Crater pollen record (Fig. 10). Of the 38, seven pollen types were identified down to genus level while one was identified to the species level and the rest to family level. Woody plants and ferns account for the vast majority of plant types identified, with an average of 107 and 106 grains, respectively, per level. Herbs and fern allies make up a lesser proportion of the present plant types with averages of 1.15 and 0.25. Gray shading represents a 10× exaggeration. The average count per level was 215 grains and spores.

The pollen record contains three major zones corresponding to depth ranges (ages). Zones 1 and 2 both have sub-zones (1A, 1B, 3A, 3B) (Fig. 10), which were created in the Tilia program using the CONISS function to generate stratigraphically constrained incremental sum-of-squares cluster analysis (Grimm 1991; Grimm 1986). The sum of squares cluster analysis minimizes total within-cluster dispersion for n groups around n centroids. The incremental sum of squares method approximates the overall optimal n groups, placing clusters in a hierarchy (Grimm 1986).

Pollen zone 1A: (315-295 cm, 7650-6800 cal yr BP)

Zone 1 contains 31 pollen types and is a tree-rich pollen assemblage with dry-to-mesic and wet-to-mesic taxa. Zone 1A has the greatest amount of Pandanaceae-*Pandanus*, Myrsinaceae-*Myrsine*, and Moraceae.

Pollen zone 1B: (295-235 cm, 6800-5500 cal yr BP)

Transitioning to zone 1B, Polypodiaceae: bilateral monolete reaches a climax, Myrtaceae and Mysinaceae-*Myrsine* decrease and Moraceae disappears. Zone 1B contains the greatest amount of Pandinaceae-*Freycinetia*, Euphorbeaceae-*Antidesma*, Violaceae and Polygonaceae.

Pollen zone 2: (235-108 cm, 5500-4525 cal yr BP)

Zone 2 has an assemblage of 32 pollen types and records more low-growing shrubs and herbs. Zone 2 has the greatest amount of Euphorbiaceae *Sandwicensis*-type, Arecaceae, Sapindaceae and Araliaceae. Considerable percentages of Chenopodiaceae, Rubiaceae-*Kadua*, Rutaceae, and Sapindaceae are found in this zone.

Pollen zone 3A: (108-65 cm, 4525-2400 cal yr BP)

Zone 3A contains 24 pollen types. Large trilete spores peak in number in this zone. The greatest abundance of Myrtaceae is also in this zone.

Pollen zone 3B: (65-35 cm, 2400-1650 cal yr BP)

Zone 3B is the least diverse zone with only 14 pollen types. Myrtaceae continues from zone 3A in large numbers. Theaceae makes its only appearance in this zone. Arecaceae and Araceae are abundant, while most other pollen types are absent.

Select taxa representative of an assortment of dry, mesic and wet precipitation ranges were evaluated in terms of influx. All taxa show a marked increased influx between 5000-6000 cal yr BP (Fig. 11). Only Myrtaceae, Araceae, Arecaceae, Pandanaceae *Freycinetia arborea* and Polypodiaceae, specifically spores with bilateral monolete morphology, trace an influx after 3000 cal yr BP.

3.3.5 Temperature and precipitation reconstructions

The dry and wet precipitation categories are the least prominent in the pollen sum. The dry, wet, dry-to-mesic and mesic precipitation categories are shown with a supplied 10× exaggeration (Fig. 12). Dry-to-wet taxa are consistent through all zones but have peaks between zones 1A and 1B, and again in zone 2. Wet and dry taxa are completely absent from zone 1A. Zone 1B shows an increase in mesic and mesic-to-wet taxa continuing into zone 2. Dry-to-mesic taxa patterns are most frequent in zones 1A and 1B. Zone 2 is predominantly composed of dry-to-wet and mesic-to-wet taxa. Mesic-to-wet taxa peak in zone 2. The greatest amount of wet taxa occurs in zone 2. Dry taxa are limited to zones 2, 3A and 3B. Zone 3A contains mostly mesic-to-wet and dry-to-wet taxa, with small amounts of dry and dry-to-mesic taxa. Mesic taxa peak in zone 3B.

Taxa with upper elevation limits between 2000-2500 m account for the majority of the pollen sum. Cool temperatures are characteristic of zone 1. Zones 1A and 1B contain the greatest percentage of cold-tolerant taxa. These taxa then disappear after zone 1B and are absent from zones 2-3. Zone 1B shows great numbers of taxa with elevation limits between 1000-1500 m and 1500-2000 m. There is a significant decrease in the taxa with upper elevation limits between 1000-1500 m throughout zone 2. Taxa confined to lowland areas are most abundant in zone 2 out of all zones, see a great decrease in zone 3A, then are absent from zone 3B. Taxa tolerant of cooler temperatures, with upper elevation limits between 2000-3000 m, appear in the latter part of zone 2 and continue into zones 3A and 3B.

Weighted averages of pollen precipitation and upper elevation limits were calculated to display overall trends (Fig. 13c, Fig. 13d). In terms of temperature, conditions appear relatively constant apart from three short-duration departures of 0.86-1.48°C between 7500 and 7200 cal yr BP; 5400 and 5000 cal yr BP; and 2000 and 1700 cal yr BP. The precipitation reconstruction displays two major trends: drier conditions in the early Holocene and a wetter late Holocene.

3.4 DISCUSSION

3.4.1 Radiocarbon dates and chronology

Two reversals occur in the Kaʻau Crater chronology, the first in the mid-Holocene and the second previous to the onset of the Holocene. This study does not consider time periods before 9000 cal yr BP, so this period in the core will not be discussed further. The bulk date of sample HWI-KAA-256 is inconsistent with the fine fraction date from the same sample; therefore it was also discarded. The age-depth curve reveals an increased accumulation rate beginning shortly after 6000 cal yr BP and lasting until approximately 4000 cal yr BP. This enhanced sediment deposition could be a result of successive mass wasting events due to torrential storms during this 2000-year period. Natural erosion agents such as wind and water could have also intensified between 6000-4000 cal yr BP, increasing sediment accumulation. An alternate interpretation is that vegetation was thriving during the wet season and undergoing major diebacks each year due to consistent drought events. It is not certain the exact cause, but these results demonstrate anomalous conditions during this time period either in Hawaiʻi or Pacific-wide.

3.4.2 Bulk density and organic matter assays

The total amount of C in peat is quantified as the product of bulk density (g/cm^3) and the carbon percentage (Chambers et al. 2011). Bulk density values in the Ka'au Crater sediment core range from 0.04 to 0.64 g/cm^3. Peat bulk density data from tropical regions are sparse, however Chambers et al. (2011) suggests peat bulk density in tropical peats tends to range from 0.05 to 2 g/cm^3. Bulk density increases twice in the Ka'au Crater record, at the onset of the Holocene and during the middle of the Holocene marking increased amounts of inorganic material and subsequently decreases in C content (Fig. 9b). Yu et al. (2003) interpreted changes in peat-core bulk density as reflecting the degree of decomposition that occurred in near surface peat. Wet and or cool conditions would then inhibit decomposition resulting in low bulk density. The Ka'au Crater ash-free bulk density record shows an overall decrease during the Holocene, coinciding with the pattern of decreasing summer insolation at 15° N (Berger and Loutre 1991). Following this rationale, Ka'au Crater may have experienced overall warmer conditions at the beginning of the Holocene followed by gradual Holocene cooling and/or drying. Periods of increased ash-free bulk density occur between 5 and 6 thousand years ago in the Ka'au profile. Wetter conditions in the crater may have encouraged increased plant production then subsequent drier conditions could have caused a mass die out and accumulation of organic matter. Hodell (2001) proposed increased seasonal insolation as causation for an altered precipitation/drought ratio in the Yucatan Peninsula over the past 2600 years. The mid-Holocene climate is characterized by pronounced changes in the insolation due to precession and obliquity (Chiang and Fang 2009). Summer insolation at 15° N reached a maximum of 474.1 w/m^2 at 10,000 cal yr BP and steadily declined throughout the Holocene to 442.5 w/m^2 at 1000 cal yr BP (Fig. 13b). The low ash-free bulk density values, compared to early-Holocene values, persisting after the mid-Holocene variable period of ash-free bulk density (6500-4800 cal yr BP) thereby suggest wetter and/or cooler conditions accompanied by periods of increased peat accumulation. Following the reasoning of Hodell (2001) decreased summer insolation values in Hawai'i could have affected the annual cycle in the Pacific and caused a wetter period from the mid- to late Holocene.

Percent LOI is variable throughout the core. A marked decrease in organic matter occurs at approximately 5900 cal yr BP, followed by high variability until about 4200 cal yr BP. This decrease may signify drought conditions and perhaps decreased plant growth, or an addition of non-organic matter to organic matter such as clastic material either blown or washed into the crater. Moy et al. (2002) argued for increased ENSO frequency after 7000 cal BP which in the Hawaiian Islands would mean increased occurrence of drought during winter months (Fig. 10h). The Kaʻau Crater pollen record (Fig. 10, Fig. 13d) suggests an increase in wet-tolerant plants after 5800 cal yr BP implying wetter crater conditions. Amplified rainfall would have supported plant taxa with high precipitation tolerance, while also increasing the inflow of non-organic material from the Kaʻau Crater walls. Bulk density values vary strongly between 5500-4500 cal yr BP with an average value of 0.20 g/cm^3. The increase in the organic matter accumulation rate (Fig. 9 g) coincides with the shift from dry to wet evident in the precipitation reconstruction (Fig. 13 b).

3.4.3 Carbon and nitrogen analyses

The Kaʻau Crater core contains relatively modest variability in ^{13}C, ranging between -26‰ and -28.5‰, just below the range of C_3 plants (-29 to -40‰) (Uchikawa et al. 2010), although two periods of differing ^{13}C values with a variable transition could be inferred (Fig. 9c). Lower ^{13}C characterize the early Holocene, 8200 to 6200 cal yr BP, while the latter half of the Holocene, 4400 to 1600 cal yr BP, traces a small increase in ^{13}C. Some variability is seen during the mid-Holocene, 6200 to 4400 cal yr BP. Increasing ^{13}C can be interpreted as a phase change from C_3 to C_4 plant dominance consequent of high temperatures, moisture stress or lower levels of carbon dioxide (Jones et al. 2010; Indermühle et al. 1999). However, the ^{13}C values for Kaʻau Crater are suggestive of C_3 plants; it is therefore unlikely that this modest change in ^{13}C is attributable to a C_3 to C_4 vegetation change. An argument may be made, however, in favor of increased ^{13}C owing to reduced stomatal conductance. Plants procure photosynthetic CO_2-C by means of stomatal opening, during which time water loss occurs (Caird et al. 2007). Most plant species have the ability to close stomata in response to water stress, therefore when stomata are opened there is an easy replenishment of ^{12}C so that the plant doesn't have to resort to the ^{13}C (Caird et al. 2007). Plants discriminate against ^{13}C during photosynthesis because of small differences in chemical and physical properties imparted by the difference in mass (O'Leary 1988). When water is a limiting factor, plants can only afford to open stomata for short periods. And because the ^{12}C is not easily replenished with closed stomata, the plant ends up using ^{13}C and enriching photosynthate in the heavy isotope. Thus, enriched ^{13}C records often indicate drought or reduced humidity. This processes, however, is situation-dependent and many explanations for the Kaʻau Crater stable carbon isotope record may be argued. Different species of plants may have intrinsic differences in their $\delta^{13}C$, while the internal conductivity of CO_2 within leaves varies between plants, both which may affect the isotopic record (Ulrich 1997).

The accumulation of heavy nitrogen occurs via numerous means, including the predominant mineralization and subsequent consumption of the light isotope by plant roots, which depletes the litter on the soil surface of ^{15}N and subsequently enriches soil organic matter $\delta^{15}N$ (Tiunov 2006). A mid-Holocene enrichment of ^{15}N in bulk sediment is evident in the Kaʻau Crater core that may have been driven by changes in the crater floor water table and differences between anaerobic and aerobic near-surface environments (Fig. 9e). If wetter or more humid conditions existed in the early Holocene, the water table would have increased; consequently the supply of oxygen in the soil would have been reduced (Inglett and Reddy 2006). Reduced available oxygen limits microbial activity and in addition the processing of nitrogen. Decreased rainfall conversely would result in a lowered crater water table and increased oxygen availability thus encouraging microbial activity. It has been shown that the water table level in Kaʻau Crater is rather sensitive and responds rapidly to increased precipitation (Fig. 1). The rise in $\delta^{15}N$ at 7000, 6500 and between 5500-2300 cal yr BP are consistent with drier conditions potentially causing periods of depressed water table and less recharge (Fig. 9e).

3.4.4 Pollen stratigraphy

A relatively diverse assemblage of plants inhabited Kaʻau Crater throughout the Holocene. Chenopodiaceae, a dry indicator, only appeared during the late mid-Holocene. Rubiaceae, a dry-mesic indicator appeared briefly at the onset of the Holocene and during the mid-Holocene while Myrsinaceae, which is tolerant of a wide range of dry to wet conditions, persisted in fairly stable amounts throughout the Holocene. Dry, dry-mesic and mesic taxa were all present between 6000 and 2500 cal yr BP, although wet taxa existed in similar numbers and mesic-to-wet taxa were much more abundant. Rubiaceae, a dry-tolerant taxa, exhibits a scattered presence in the Ka‘au Crater pollen record while another dry taxa, Polypodiaceae, is consistent in numbers throughout the entire core in partial support of Hypothesis 2a.

Pritchardia pollen is particularly significant in this pollen record as its change in abundance throughout the core indicates a major shift from drier conditions in the early Holocene to wetter conditions from the mid to late Holocene. *Pritchardia* is absent from zone 1 then appears and maintains in great numbers through zones 2 and 3 (Fig. 10). Hotchkiss and Juvik (1999) found that *Pritchardia* had been a major component of upland vegetation assemblages on O‘ahu since about 19,368 cal yr BP; however, they saw a decline in *Pritchardia* at 13,271 cal yr BP and 11,129 cal yr BP. The later portion of Hotchkiss and Juvik's (1999) pollen record contained pollen assemblages depicting mesic-to-wet forests with less *Pritchardia* and more *Metrosideros*-type pollen from the beginning of the Holocene to about 8120 cal yr BP. The pollen record from this study continues to trace the decline in *Pritchardia* in the early Holocene, but also captures a mid-Holocene re-population of *Pritchardia*. The combined Ka‘au Crater records detail an important vegetation reaction to climate translated as a wetter period following the last glacial maximum, a drier early Holocene, with wetter conditions once again mid- to late Holocene.

3.4.5 Temperature and precipitation reconstructions

The climatic interpretation of the pollen record shows a relatively consistent temperature with a modest cooling trend throughout the Holocene, likely influenced by the decreasing summer insolation (Fig. 13c), with marked warm departures of 1.17-1.48°C, at 7510, 6690, 5400 and 1980 cal yr BP, evident in increases in pollen taxa such as Pandanaceae *Pandanus* and Euphorbiaceae *Claoxylon sandwicense* with upper elevation limits between 0-1000 m. Temperature briefly increases once again later in the Holocene by about 0.86°C according to an increase in pollen taxa with upper elevation limits between 1000-2000 m such as Urticaceae and Pandanaceae *Freycinetia arborea*.

The precipitation reconstruction reveals variation on multi-millennial and shorter scales. A drier period appears from about 8000 cal yr BP to about 5600 cal yr BP (Fig. 13d). At this point, a major departure occurs shifting to wetter conditions persisting from about 5400 to 1650 cal yr BP indicated by increasing numbers of mesic-to-wet and wet taxa. These results are consistent with those of Burney et al. (1995), who found a two-to four-fold precipitation increase between 5800 and 2200 cal yr BP. Burney proposed that an upward shift of the upper boundary of the cloud layer associated with the mid-Pacific Trade Wind Inversion caused the increase in rainfall at Flat Top Bog. The TWI in Hawai‘i sits at about 2200 m (Giambelluca et al. 2011), therefore, if the upper limits of the TWI did increase around 5800 cal yr BP, as Burney proposed, then Ka‘au Crater, 460 m, also may have been affected. Moreover, the mechanisms which affect trade wind height such as sea surface temperature, divergence, surface wind speeds, and the North Pacific anticyclone may have caused conditions under which orographic lifting hence precipitation increased both at Flat Top Bog and Ka‘au Crater (Albrecht 1984; Giambelluca and Nullet 1991).

The increased precipitation at Ka‘au Crater during the mid-Holocene also agrees with Barron and Anderson's (2011) suggestion of suppressed El Niño conditions between 8000-4000 cal yr BP. Barron and Anderson's (2011) data compilation offers that during the mid-Holocene, the Aleutian Low was generally weaker during the winter and the North Pacific generally resembled a La Niña-like or more negative PDO phase. Oxygen isotope ratios of bulk sediment (pure micrite) calcite from Jellybean Lake also record Aleutian Low storm paths above and near the coastal mountains, suggesting a weaker or more westward Aleutian Low between 8000 and 4500 cal yr BP (Fig. 13i) (Anderson et al. 2006).

The degree of insolation was another factor in a state of change throughout the Holocene. Kirov and Georgieva (2002) demonstrated that large-scale phenomena orchestrating global climate such as ENSO undergo long-term variations closely related to the secular solar activity variations. From the onset of the Holocene, mid-month December insolation values at 20° N were consistently increasing while mid-month July insolation values at 20° N were decreasing (Fig. 13a, Fig. 13b) (Berger and Loutre 1991). In the Pacific region, increased insolation equates to a decrease in pressure of both the Aleutian Low and the Hawaiian High, a westward shift in the longitude of the Aleutian Low and an eastward shift of the Hawaiian High (Kirov and Georgieva 2002). The opposite effects occur with decreased solar activity. These changes would have meant more El Niño-like conditions during winter months in the Northern hemisphere and more La Niña-like conditions during the summer months, both intensifying as the Holocene progressed. The increase and decrease of solar insolation in December and June, respectively, may have intensified seasonal variations in Hawaiʻi in terms of El Niño in the winter and La Niña in the summer. If this were the case, vegetation experienced optimal growing conditions for much of the year and disadvantageous circumstances the rest perhaps resulting in increased organic matter accumulation in Kaʻau Crater.

Firing et al. (2004) noted that comparison with National Centers for Environmental Prediction (NCEP) reanalysis wind and pressure shows that high (low) sea level phases around Hawaiʻi are associated with an increase (decrease) in the strength of the Aleutian low. While the correlation between sea level and ENSO in Hawaiʻi is not confidently known, Firing et al. (2004) showed that Hawaiʻi sea level is correlated with sea surface height (SSH) over a significant portion of the North Pacific Ocean, and with the Pacific–North America (PNA) index, which represents teleconnections between tropical and midlatitude atmospheric variations. Association of higher sea levels in Hawaiʻi during El Niño may be drawn from Polovina et al. (1994) who illustrated that similar variability as Hawaiʻi occurs along the North American coast in San Francisco and San Diego, California, tide gauge records (Firing et al. 2004). Therefore, if El Niño is associated with a strengthening of the Aleutian low, then it is likely that a weaker Aleutian Low and La Niña-like conditions were plausible during the mid-Holocene.

Uchikawa et al. (2010) found changes in the mean stable carbon value of leaf waxes ($\delta^{13}C_{alk}$) in a core from Ordy Pond on coastal Oʻahu indicating changes in vegetation structure through the Holocene. They interpreted these results as increased aridification (decreased moisture) and a shift from C_3 to C_4 plants in response to climate shifts. The variability in the Kaʻau Crater records between 6000 and 4000 cal yr BP are in agreement with a sudden enriched departure in $\delta^{13}C_{alk}$ observed during this time by Uchikawa et al.

(2010), and consistent with a number of other records from throughout the Hawaiian Islands (Athens 1997; Burney and Burney 2003). Burney and Burney (2003) found charcoal peaks in their charcoal particle stratigraphies fro Kauaʻi, Hawaiʻi between 4080-4290cal yr BP and associated this with prolonged drought conditions. One of Burney and Burney's nine cores from the Māhāʻulepū Cave System taken from the center of the sinkhole contains a pre-human charcoal peak beginning 475 cm below surface and continues up to about 50 cm of sediment. The initiation of charcoal increase is recorded only at this location (of the three sites in the cave) and occurs around 4290 cal yr BP, suggesting that this site was the only one receiving sediment at that time, as a result of low-water conditions (Burney and Burney 2003). Using a coupled general circulation model, Uchikawa et al. (2010) documented an overall drying trend in Hawaiʻi from 10,000 cal yr BP to present. The simulated sea surface temperature from their modeling exercise showed continuous winter warming of the equatorial cold tongue, intensification of the Hadley circulation and a strengthening of surface trade winds in the northern subtropics. The combination of these processes, they proposed, reduced the transport of moist tropical air to the Hawaiian Islands thus causing a drying pattern. The precipitation reconstruction from Hotchkiss and Juvik's (1999) Kaʻau Crater record is in agreement with the model results of Uchikawa et al. (2010), showing wetter conditions leading into and persisting in the Holocene (Fig. 13d). The precipitation reconstruction from this study shows greater precipitation amounts during the overlap with Hotchkiss and Juvik's (1999) record, although exhibits a drying trend from approximately 7200 to 5800 cal yr BP (Fig. 13d). Precipitation increases abruptly after 5800 cal yr BP and maintains a pattern of overall greater values than the early Holocene. The latter half of the Kaʻau Crater precipitation reconstruction falls in line with Rooney et al.'s (2004) results which recorded the most recent reef accretion on Molokaʻi, Kailua and Punaluʻu on Oʻahu occurring between 4900-5600 cal yr BP. The major reduction in reef accretion, they reason, is a result of increased wave energy associated with El Niño. Greater wave activity is often accompanied by precipitation, especially during winter month in the Hawaiian Islands, thus rainfall at Kaʻau Crater may have increased during this mid-Holocene wave energy increase.

The records from Kaʻau Crater portray climate and vegetation dynamics at a mountaintop location, which may be applied to similar areas throughout the Pacific region.

Natural vegetation in the Crater is seen to be sensitive to climate. This understanding is one, which shouldn't be overlooked, as climate change today and in the future will likely be felt by native plant communities. The habitats and distribution of invasive species are further circumstances that likely will alter mountain vegetation. Invasive species harm native vegetation while costing natural resource programs time and money. Human driven expansion in the islands is yet another factor affecting vegetation as well as watershed functions. Land-use change and development often alter drainage patterns and put stress on water resources. As seen in the precipitation reconstruction for Kaʻau Crater, dry conditions can appear somewhat suddenly and last for a long time. Without proper planning and management, drought may cause severe water-shortages to already taxed island water supplies.

3.5 SUMMARY AND CONCLUSIONS

The overarching aim of this research was to gain insight on past vegetation and rainfall dynamics at Kaʻau Crater in order to better understand implications of current and future climate change. Specifically, this study examined recent rainfall patterns across three mountaintop locations on Oʻahu, reconstructed vegetation population dynamics in Kaʻau Crater through the Holocene, and lastly, produced precipitation and temperature reconstructions based on the vegetation record. It was found that Kaʻau Crater, receives moderate rainfall throughout most years compared to Poamoho and Kaʻala. Due to its windward location, Kaʻau Crater receives greater mean rainfall annually than Kaʻala; however, because it is lower in elevation, receives less annual rainfall on average than Poamoho. Kaʻau Crater is slightly more responsive to PDO phase-change; this signifies that long-term alterations in atmospheric circulation may be evidenced in paleoclimatic records from Kaʻau Crater. In terms of vegetation in and around Kaʻau Crater, a number of species that currently inhabit the crater were at some point present during the Holocene such as Myrtaceae *Metrosideros polymorpha*, Cyperaceae, and Myrtaceae. The precipitation reconstruction suggests drier conditions in the crater from the onset of the Holocene until approximately 5800 cal yr BP when a dramatic shift to wetter conditions occurred. These results indicate primarily, that precipitation at Kaʻau Crater may vary on millennial time scales, and secondly, that a reorganization of atmospheric circulation may cause abrupt changes in terms of temperature and precipitation at the crater.

Table 1. Climatic interpretation of pollen types found in the Ka'au Crater pollen record. Elevation limits, precipitation ranges and pollen abundance index (PAI) values are from Hotchkiss and Juvik (1999).

POLLEN TYPE	Lower elevation limit (m)	Upper elevation limit(m)	Precipitation range	PAI Temp (°C)	PAI Precip (mm)
AMARANTHACEAE	110	1750	Mesic-Wet	r	r
ARALIACEAE	30	2190	Dry-Wet	15.4	3000
CHENOPODIACEAE	0	2750	Dry	x	1000
EPACRIDACEAE	15	3230	Dry-Wet	x	x
ERICACEAE	500	3700	Dry-Wet	x	x
EUPHORBIACEAE: Antidesma	300	1100	Dry-Wet	18.3	5000
EUPHORBIACEAE: Claoxylon sandwicense	550	650	Dry-Wet	r	r
EUPHORBIACEAE-type	-	-	Dry-Wet	r	r
FABACEAE: Acacia koa	60	2060	Dry-Wet	x	x
GESNERIACEAE	100	1900	Mesic-Wet	r	r
GUNNERACEAE	920	1520	Wet	r	r
LOGANIACEAE	270	1550	Mesic-Wet	r	r
MALVACEAE: Hibiscus-type	0	1310	Dry-Wet	19.1	600
MORACEAE	300	1680	Dry-Mesic	15.5	4900
MYRSINACEAE: Myrsine	215	2200	Dry-Wet	13.7	x
MYRTACEAE: Metrosideros-type	0	2200	Dry-Wet	x	x
PLANTAGINACEAE	480	2200	Wet	x	x
POLYGONACEAE	180	3050	Dry-Wet	x	900
RUBIACEAE: Coprosma	270	2590	Dry-Wet	x	x
RUBIACEAE: undifferentiated	0	2070	Dry-Wet	x	2000
RUTACEAE : Melicope type 1	300	2060	Dry-Wet	13.5	4000
RUTACEAE: Platydesma	340	1420	Wet	r	r
THEACEAE	450	1600	Wet	r	r
THYMELAEACEAE	0	2290	Dry-Wet	19.2	x
SAPINDACEAE	3	2350	Dry-Mesic	x	1750
URTICACEAE: Pilea	40	1950	Mesic-Wet	r	r
URTICACEAE: Pipturus-type	60	2400	Dry-Wet	19.0	1500
URTICACEAE: Urera	150	1700	Mesic-Wet	r	r
VIOLACEAE	330	2010	Mesic-Wet	r	r
ARACEAE	-	-	Mesic	r	r

Table 1. *Continued*

ARECACEAE: Pritchardia	0	2000	Mesic-Wet	18.9	5500
CYPERACEAE	-	-	Dry-Wet	x	x
LYCOPODIACEAE	-	-	Mesic-Wet	15.4	4000
PANDANACEAE: Freycinetia arborea	300	1500	Mesic-Wet	18.4	2000
PANDANACEAE: Pandanus	0	610	Mesic-Wet	23.4	2500
POACEAE	0	4090	Dry-Wet	x	x
GLEICHENIACEAE	-	-	Mesic-Wet	x	x
HYMENOPHYLLACEAE	-	-	Wet	r	r
POLYPODIACEAE	-	-	Dry-Wet	14.6	3000

*Lower and upper elevation limits are from Hotchkiss and Juvik (1999) and Wagner et al. (1990). Precipitation ranges are also from Hotchkiss and Juvik (1999), originally found in Gagné and Cuddihy (1990) and Wagner et al. (1990). Precipitation ranges are reported in six categories: dry (0–1200 mm average annual precipitation), dry-to-mesic (<2500 mm), mesic (1200–2500 mm), mesic-to-wet (>1200 mm), wet (>2500 mm), and dry-to-wet (<1200 to >2500 mm). Pollen abundance index (PAI) values are the mean annual temperature (°C) and median annual precipitation (mm) of the surface sample with the highest observed percentage of each pollen type, from a collection of 102 surface samples from the island of Hawai'i (Hotchkiss and Juvik 1999). Hotchkiss and Juvik (1999) did not include values for certain pollen types because they were too rare in the surface sample collection (r), or because values >40% of the greatest observed value occurred in samples ranging 4°C in mean annual temperature or 2500 mm in median annual precipitation (x).

Table 2. Seventeen samples from the Ka'au Crater core were radiocarbon dated. Radiocarbon ages were calibrated to calendar years BP using the program Calib Rev 6.1.0, which employs the IntCal09 calibration curve (Reimer et al. 2010).

Laboratory identification (UBANo)	Sample ID	Sample type	Depth (cm)	Radiocarbon age (^{14}C yr BP)	Calibrated age (cal yr BP)
UBA-18793	HWI-KAA-32	b.s.	31-32	1726 ± 26	1638
UBA-11869	HWI-KAA-64	b.s.	63-64	2302 ± 27	2335
UBA-18794	HWI-KAA-90	b.s.	89-90	3640 ± 28	3952
UBA-11876	HWI-KAA-128	f.f.	127-128	4228 ± 29	4817
UBA-11870	HWI-KAA-128	b.s.	127-128	4158 ± 25	4704
UBA-18795	HWI-KAA-163	b.s.	162-163	5447 ± 33	6245
UBA-11871	HWI-KAA-192	b.s.	191-192	4677 ± 25	5395
UBA-11877	HWI-KAA-256	f.f.	255-256	5290 ± 32	6079
UBA-11872	HWI-KAA-256	b.s.	255-256	4859 ± 32	5601
UBA-18796	HWI-KAA-288	b.s.	287-288	5973 ± 34	6810
UBA-11873	HWI-KAA-320	b.s.	319-320	7109 ± 28	7945
UBA-18797	HWI-KAA-358	b.s.	357-358	11107 ± 50	12998
UBA-12127	HWI-KAA-384	f.f.	383-384	12127 ±39	13970
UBA-12235	HWI-KAA-384	b.s.	383-384	12235 ± 38	14087
UBA-18798	HWI-KAA-413	b.s.	412-413	10801 ± 48	12678
UBA-11875	HWI-KAA-430	b.s.	429-430	10914 ± 37	12777
UBA-18799	HWI-KAA-442	b.s.	441-442	10010 ± 55	11499

*Seventeen samples were radiocarbon dated from the 450 cm sediment core. Three of the seventeen samples were fine fraction and the rest were bulk sediment. Radiocarbon dates were calibrated using program Calib Rev 6.1.0 (Stuiver and Reimer 1993) which uses the IntCal09 calibration curve (Reimer et al. 2010).
**Bulk sediment: b.s.; fine fraction: f.f.
***Calibrated ages are median probability

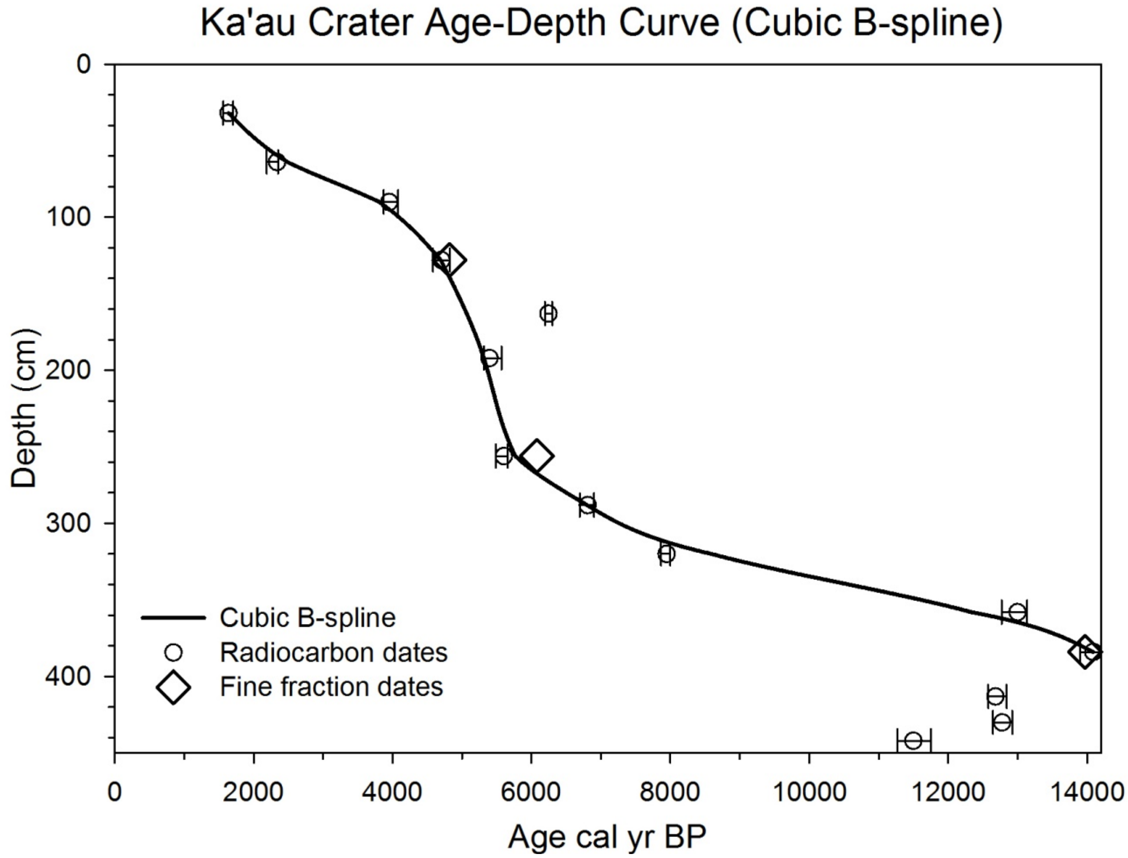

Fig. 8. Cubic B-spine age-depth curve for the Ka‘au Crater core created in the Tilia program using calibrated radiocarbon bulk sediment dates.
*Error bars represent the 2-sigma ranges

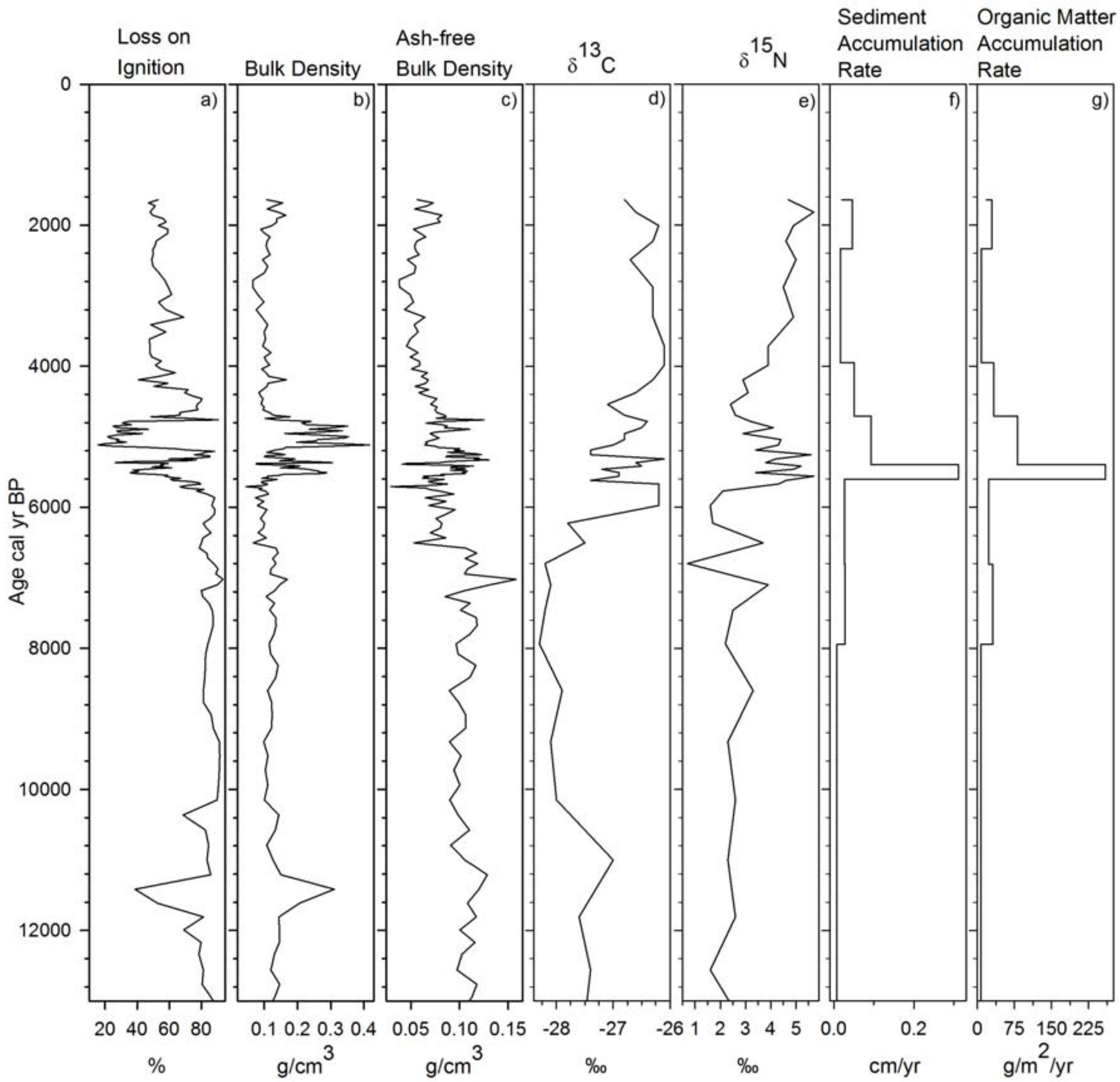

Fig. 9. Kaʻau Crater a) percent loss on ignition; b) bulk density; c) ash-free bulk density; d) delta ^{13}C content; e) delta ^{15}N content; f) sediment accumulation rate; and g) organic matter accumulation rate.

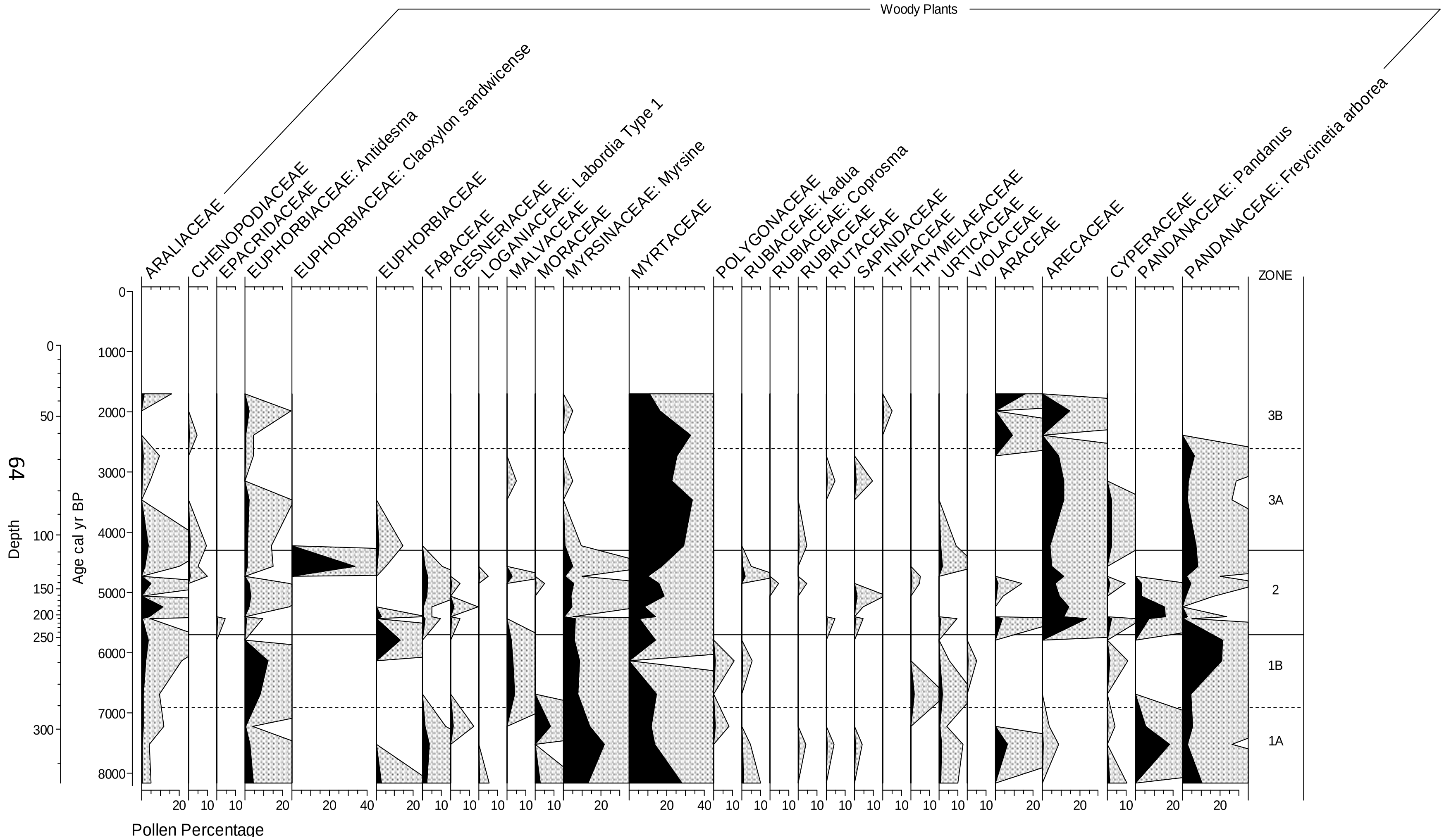

Fig. 10. Ka'au Crater pollen percentage diagram.

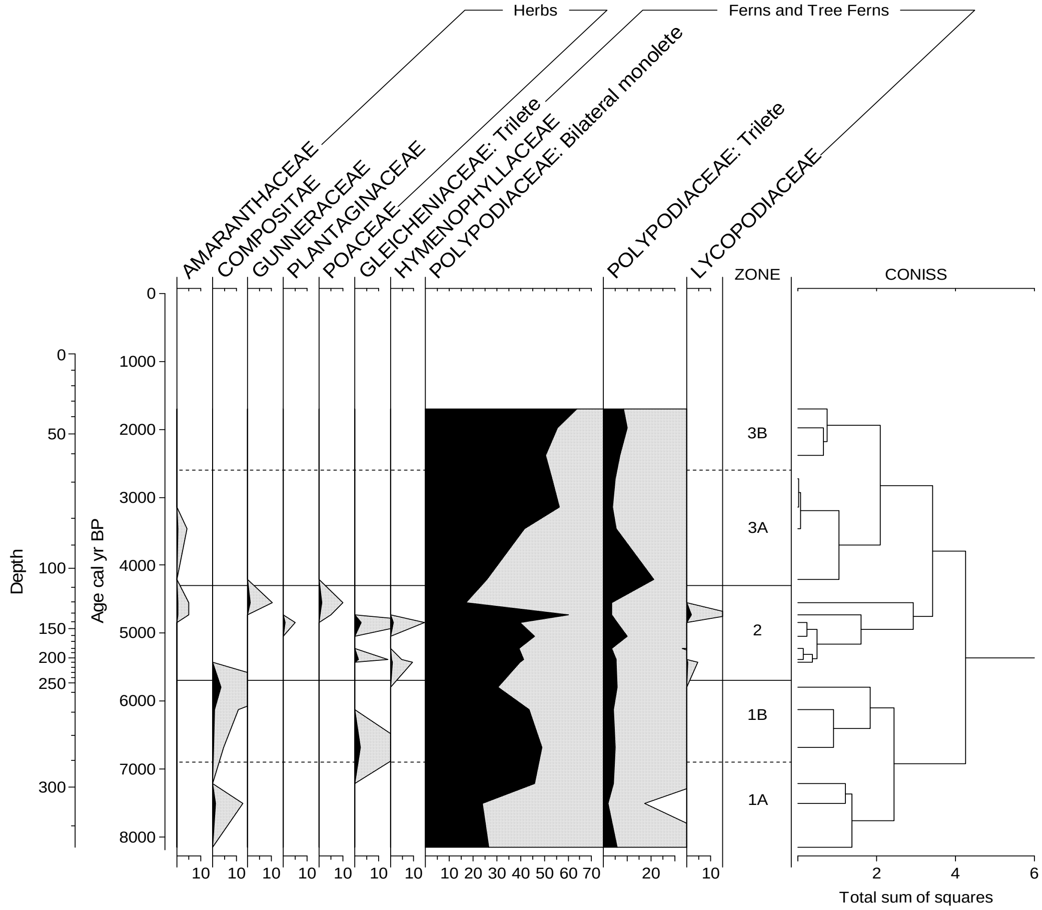

Fig. 10. *Continued*

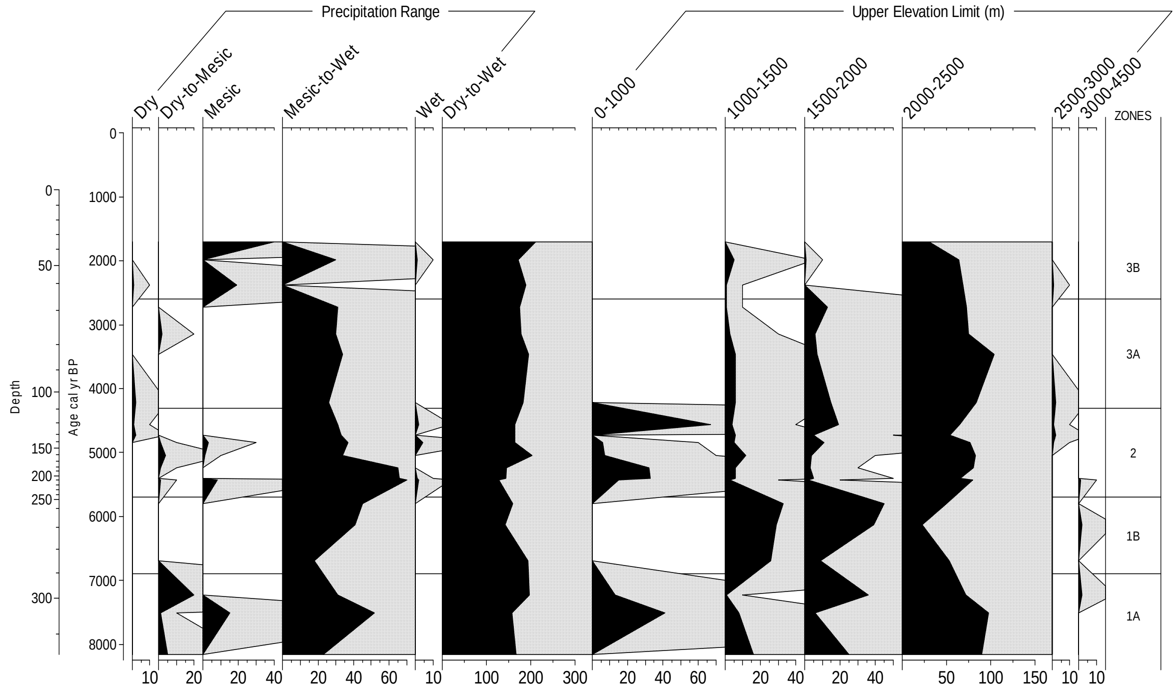

Fig. 11. Temperature and precipitation percentage reconstructions were created by taking the weighted mean of each precipitation range group and upper elevation range group.

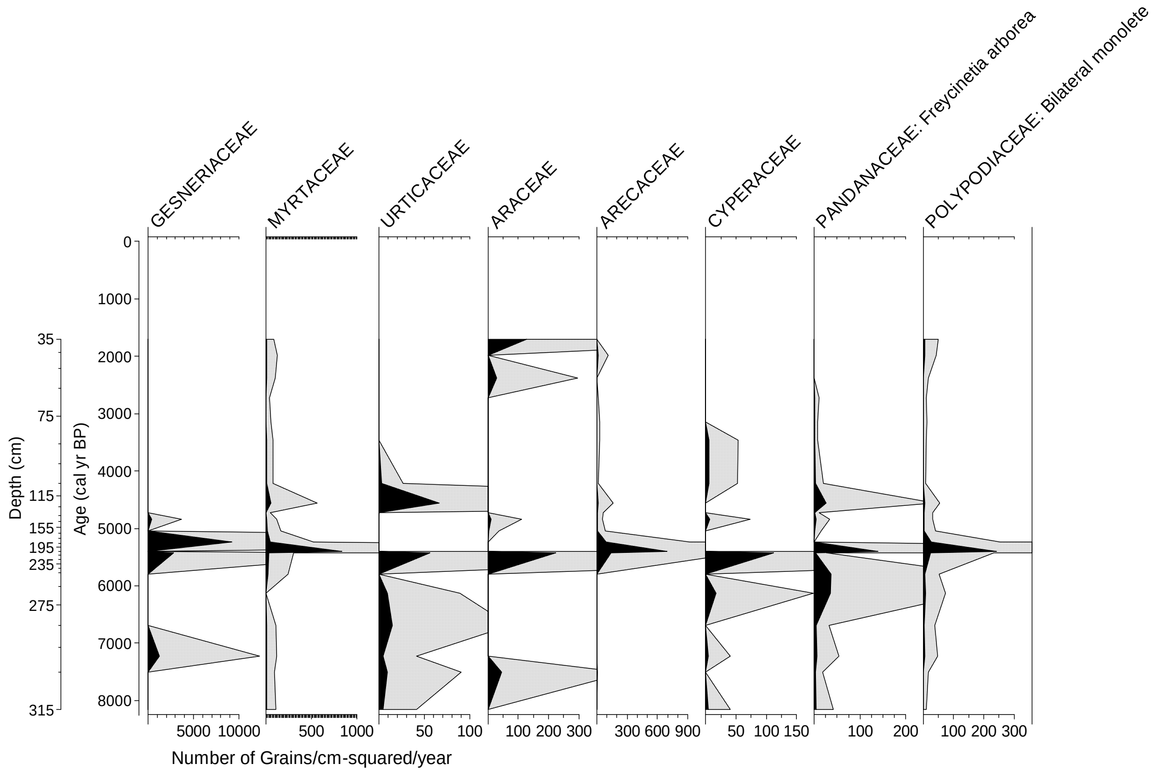

Fig. 12. Ka'au Crater pollen influx diagram.

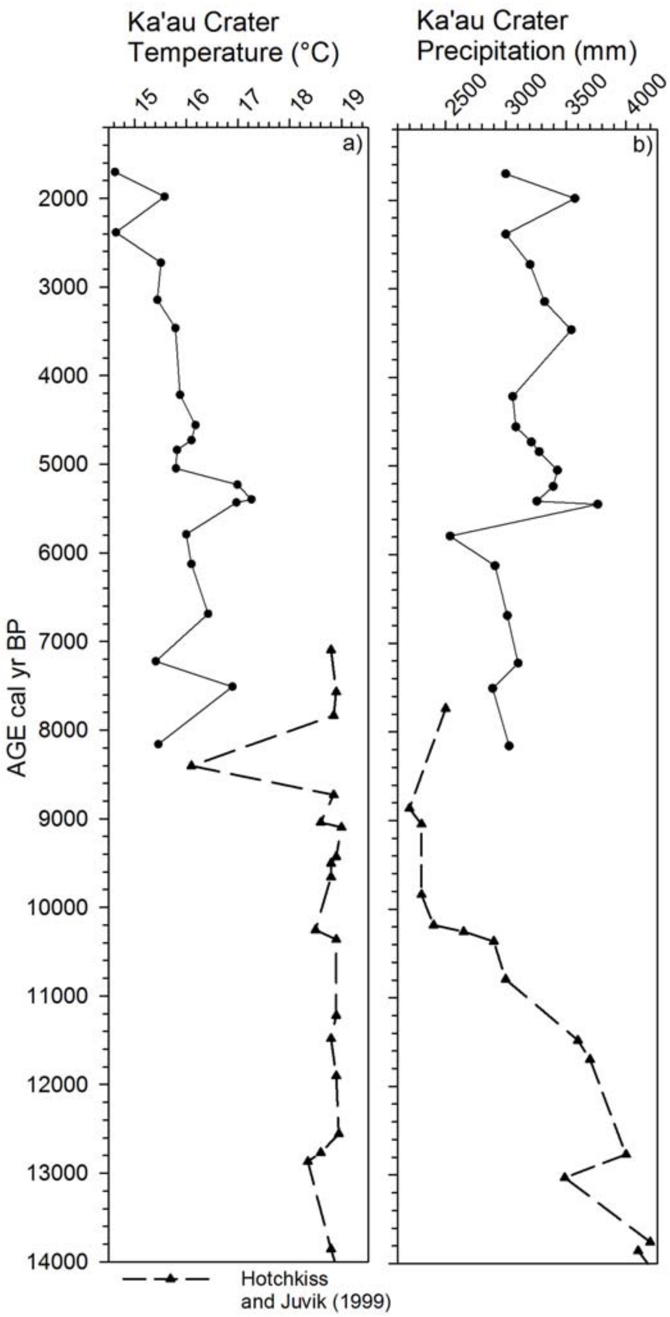

Fig. 13. Temperature and precipitation reconstructions for Ka'au Crater.

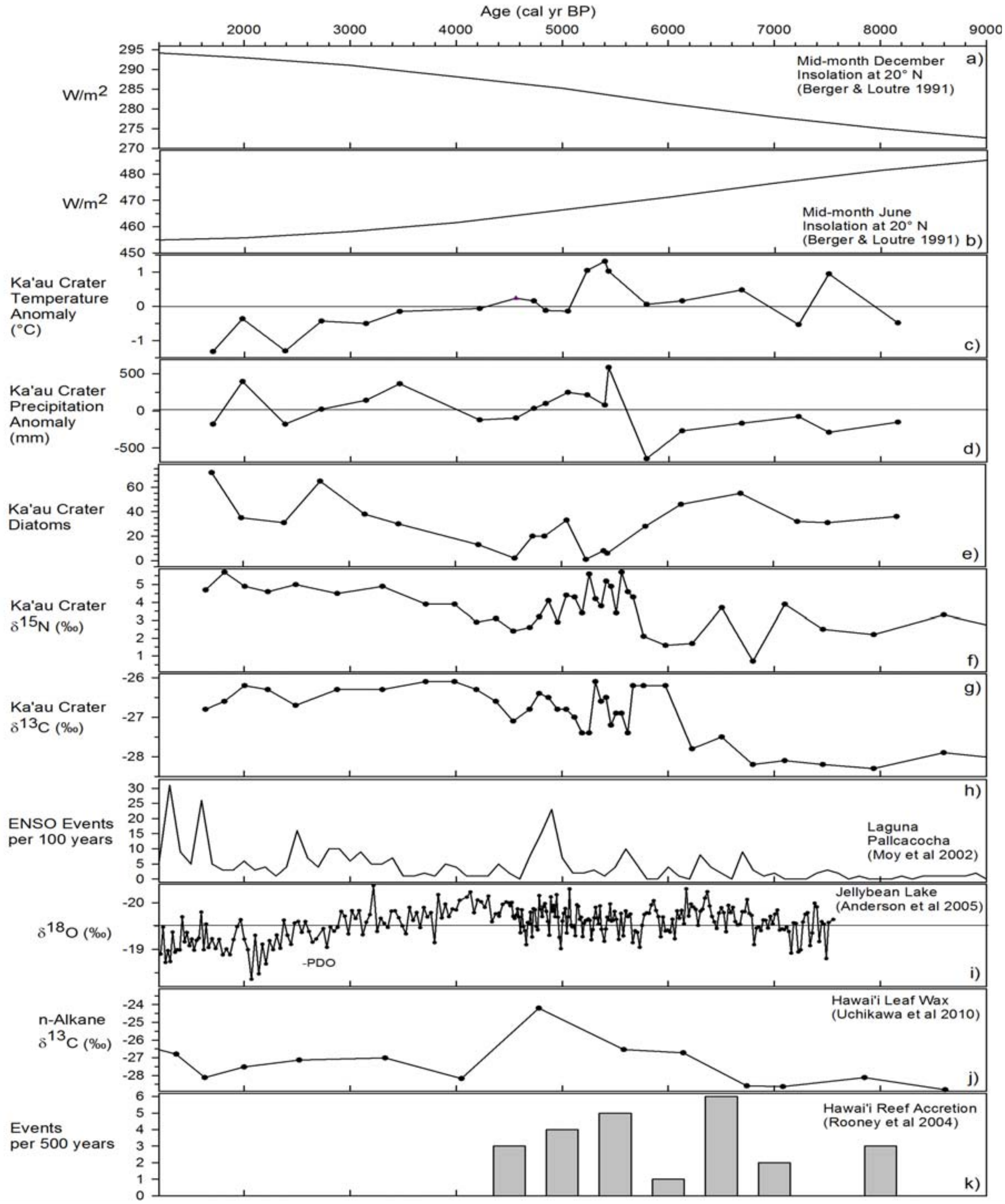

Fig. 14. a) Mid-month December insolation values for 20° N from Berger and Loutre (1991); b) mid-month June insolation values for 20° N from Berger and Loutre (1991); c) temperature anomaly for Ka'au Crater; d) precipitation anomaly for Ka'au Crater; e) diatom abundance throughout the Ka'au Crater core; f) delta ^{15}N values for Ka'au Crater; g) delta ^{13}C values for Ka'au Crater; h) Moy et al. (2002) ENSO events in a 100-yr overlapping window from Ecuador; i) Anderson et al. 's (2005) delta ^{18}O record from southwestern Yukon; j) n-Alkane record of leaf wax from Uchikawa et al. (2010); k) total reef accretion events per 500 years in Hawai'i (Rooney et al. 2004).

3.6 LITERATURE CITED

Albrecht, B.A., 1984: A model study of downstream variations of the thermodynamic structure of the trade winds. *Tellus*, 36A, 187–202

Anderson, L., Abbott, M.B., Finney, B.P., Burns, S.J. 2006. Erratum to "Regional atmospheric circulation change in the north Pacific during the Holocene inferred from lacustrine carbonate oxygen isotopes, Yukon Territory, Canada". *Quaternary Research* 65, 350-351.

Athens, J.S. 1997. Hawaiian native lowland vegetation in prehistory. Pages 248-270 in P.V. Kirch and T.L. Hunt, eds. *Historical ecology in the Pacific Islands*. Yale University Press, New Haven, Connecticut.

Athens, S.J., and Ward, J.V. 1993. Environmental Change and Prehistoric Polynesian Settlement in Hawai'i. *Asian Perspectives* 32(2), 205-223.

Athens, J.S., Ward, J.V., and Wickler, S. 1992. Late Holocene lowland vegetation, O'ahu, Hawai'i. *New Zealand Journal of Archaeology* 14, 9–34.

Athens, J.S., Ward, J.V., and Tomonari-Tuggle, M.J. 1996. Archaeological inventory survey and paleoenvironmental coring for kiosks, boardwalk and parking areas, Kealia Pond National Wildlife Refuge, Kihei, Maui, Hawai'i. International Archaeological Research Institute, Inc.

Barron, J.A., and Anderson, L. 2011. Enhanced Late Holocene ENSO/PDO expression along the margins of the eastern North Pacific. *Quaternary International* 235, 3-12.

Berger, A., and Loutre M.F. 1991. Insolation values for the climate of the last 10 million of years. *Quaternary Sciences Review* 10(4), 297-317.

Brady, N.C., and Weil, R.R. 2002. *The Nature and Properties of Soils*. New Jersey: Prentice Hall, 960 pp.

Burney, D.A., DeCandido, R.V., Burney, L.P., Hostel-Hughes, F.N., Stafford Jr., T.W., and James, H.F. 1995. A Holocene record of climate change, fire ecology and human activity from montane Flat Top Bog, Maui. *Journal of Paleolimnology*, 13.3.

Burney, L.P., and Burney, D.A. 2003. Charcoal stratigraphies for Kaua'i and the timing of human arrival. *Pacific Science* 57, 211-226.

Caird, M.A., Richards, J.H., and Donovan, L.A. 2007. Nighttime stomatal conductance and transpiration in C-3 and C-4 plants. *Plant Physiol.* 143, 4–10.

Cane, M.A. 1998. A role for the tropical Pacific. *Science* 282, 59–61.

Chambers, F.M., Beilman, D.W., and Yu, Z. 2011. Methods for determining peat humification and for quantifying peat bulk density, organic matter and carbon content for palaeo studies of climate and peatland carbon dynamics. *Mires and peat* 7, 1-10.

Charman, Dan. *Peatlands and environmental change.* West Sussex, England: John Wiley and Sons Ltd., 2001. Print.

Chesworth, Ward. *Encyclopedia of soil science.* Dordrecht, Netherlands: Springer, 2008. Print.

Chiang, John C.H. 2009. The Tropics in Paleoclimate. *Annual Review of Earth and Planetary Sciences* 37, 263-297.

Chiang, J.C.H, and Fang, Y. 2009. Pacific Climate Change and ENSO Activity in the Mid-Holocene. *American Meteorological Society* 22, 923-939.

Crausbay, S.D. 2011: Vegetation-climate relationships across space and time at high elevation in Hawai'i. Ph.D. thesis, Department of Botany, University of Wisconsin, Madison, 177 pp.

Dean, W.E. 1974. Determinations of carbonate and organic matter in calcareous sediments and sedimentary rocks by loss on ignition; comparison with other methods. *Journal of Sedimentary Research* 44, 242-248.

Driessen, P. M.. *Lecture notes on the major soils of the world.* Rome: Food and Agriculture Organization of the United Nations, 2001. Print.

Edwards, K.J. 1983. Quaternary palynology: consideration of a discipline. *Progress in Physical Geography* 7, 113-125.

Elliot, M.E., and Hall, E.M. 1977. Wetlands and wetland vegetation of Hawai'i. U.S. Army Corps of Engineers, Pacific Ocean Division.

Faegri, K., and Iversen, J. 1989. "Textbook of Pollen Analysis" (K. Faegri, P. E. Kaland, and K. Krzywinski, Eds.), 4th ed., Wiley, New York.

Firing, Y.L., Merrifield, M.A., Schroeder, T.A., and Qiu, B. 2004. Interdecadal Sea Level Fluctuations at Hawai'i. *Journal of Physical Oceanography* 34, 2514-2524.

Foote, Donald E. and the United States Department of Agriculture Soil Conservation Service. 1972. Soil Survey of Islands of Kaua'i, O'ahu, Maui, Moloka'i, and Lana'i, State of Hawai'i. Washington, D.C., U.S. Govt. Printing Office.

Gagné, W.C., and Cuddihy, L.W. 1990. Vegetation, p 45-114. *In*: W.L. Wagner, D.R. Herbst and S.H. Sohmer, Manual of the Flowering Plants of Hawai'i. Univ. of Hawai'i. Press, Bishop Museum Press, Honolulu, HI.

Garza, J.A., Chu, P.-S., Norton, C.W., and Schroeder, T.A. 2012. Changes of the prevailing trade winds over the islands of Hawaiʻi and the North Pacific. Journal of Geophysical Research 117, D11109.

Giambelluca, T., Chen, Q., Frazier, A.G., Price, J.P., Chen, Y.-L, Chu, P.-S., Eischeid, J., and Delparte, D. (2011). The Rainfall Atlas of Hawaiʻi.

Giambelluca, T.W., and Nullet, D. 1991. Influence of the trade-wind inversion on the climate of a leeward mountain slope in Hawaiʻi. *Climate Res.* 1, 207–216.

Grand, M., and Gaidos, E. 2010. Methane Emission from a Tropical Wetland in Kaʻau Crater, Oʻahu, Hawaiʻi. *Pacific Science* 64(1), 57-72.

Grimm, E.C. 1986. CONISS: A Fortran 77 program for stratigraphically constrained cluster analysis by the method of incremental sum of squares. *Computers and Geosciences* 13(1), 13-35.

Grimm, E.C., 1991. TILIA and TILIAGRAPH. Illinois State Museum, Springfield.

Heiri, O., Lotter, A.F., and Lemcke, G. 2001. Loss on ignition as a method for estimating organic and carbonate content in sediments: reproducibility and comparability of results. *Journal of Paleolimnology* 25, 101-110.

Hodell, D.A. 2001. Solar Forcing of Drought Frequency in the Maya Lowlands. *Science* 292, 1367.

Högberg, P. 1997. 15N natural abundance in soil-plant systems. *New Phytologist* 137, 179-203.

Hotchkiss, S., and Juvik, J.O. 1999. A late-Quaternary pollen record from Kaʻau Crater, Oʻahu, Hawaiʻi. *Quaternary Research* 52, 115-128.

Indermühle, A., Stocker, T.F., Joos, F., Fischer, H., Smith, H.J., Wahlen, M., Deck, B., Mastroianni, D., Tschumi, J., Blunier, T., Meyer, R. and Stauffer, B. 1999. Holocene carbon-cycle dynamics based on CO_2 trapped in ice at Taylor Dome, Antarctica. *Nature* 398, 121-126.

Inglett, P.W., and Reddy, K.R. 2006. Investigating the use of macrophyte stable C and N isotope ratios as indicators of wetland eutrophication: Patterns in the P-affected Everglades. *Limnol. Oceanogr.* 51, 2380–2387.

Jauhiainen, J., Takahashi, H., Heikkinen, J., Martikainen, P., and Vasanders, H. 2005. Carbon fluxes from a tropical peat swamp forest floor. *Global Change Biology* 11, 1788-1797.

Jones, M.C., Peteet, D.M., and Sambrotto, R. 2010. Late-glacial and Holocene $\delta^{15}N$ and $\delta^{13}C$ variation from a Kenai Peninsula, Alaska peatland. *Palaeogeography, Palaeoclimatology, Palaeoecology* 293, 132-143.

Kennedy, E. 1975. Kaʻau Crater: A study of plant patterns in a Hawaiian bog. Unpublished MA Dissertation, 1975. University of Hawaiʻi.

Kirov, B., and Georgieva, K. 2002. Long-term variation and interrelations of ENSO, NAO and solar activity. *Physics and Chemistry of the Earth* 27, 441-448.

MacDonald, G.A., Abbott, A.T., and Peterson, F.L. 1983. Volcanoes in the Sea. University of Hawaiʻi Press, Honolulu.

MacDonald, G., and Edwards, K. 1991. Holocene palynology: I principles, population and community ecology, palaeoclimatology. *Progress in Physical Geography* 15(3), 261-289.

Moy, M., Seltzer, G., Rodbell D., and Anderson, D. 2002. Variability of El Niño/Southern Oscillation activity at millennial timescales during the Holocene epoch. *Nature* 420.

O'Leary, M.H. 1988. Carbon Isotopes in Photosyntehsis. *BioScience* 5, 328-336.

Pau, S., MacDonald, G.M., and Gillespie, T.W. 2012. A dynamic history of climate change and human impact from Kealia Pond, Maui, Hawaiian Islands. *Annals of the Association of American Geographers* 102, 748-762.

Polovina, J.J., Mitchum, G.T., Graham, N.E. Craig, M.P., Demartini, E.E. and Flint, E.N. 1994. Physical and biological consequences of a climate event in the central North Pacific. *Fish.Oceanogr,* 3, 15–21.

Prentice, I.C. 1988. Records of vegetation in time and space: the principles of pollen analysis. In: B. Huntley and T. Webb III (eds), *Vegetation History*, Kluwer Academic Publishers, Dordrecht, 16-42.

Reimer, P.J., Baillie, M.G.L., Bard, E., Bayliss, A., Beck, J.W., Blackwell, P.G.,Ramsey, C. Bronk, Buck, C.E., Burr, G.S., Edwards, R.L., Friedrich, M., Grootes, P.M., Guilderson, T.P., Hajdas, I., Heaton, T.J., Hogg, A.G., Hughen, K.A., Kaiser, K.F., Kromer, B., McCormac, F.G., Manning, S.W., Reimer, R.W., Richards, D.A., Southon, J.R., Talamo, S., Turney, C.S.M., van der Plicht, J., and Weyhenmeyer, C. E. 2010. IntCal09 and marine09 radiocarbon calibration curves, 0-50,000 years cal BP. *Radiocarbon* 51, 1111-1150.

Richardson, J.L., and Vepraskas, Michael J. *Wetland soils: genesis, hydrology, landscapes, and classification*. Boca Raton, Fla.: Lewis Publishers, 2001. Print.

Ripperton, J.C., and Hosaka, E.Y. 1942. Vegetation Zones of Hawaiʻi. 62 p. Honolulu (HI): University of Hawaiʻi. (Bulletin; B-089).

Rooney, J., Fletcher, C., Grossman, E., Engels, M., and Field, M. 2004. El Niño Influence on Holocene Reef Accretion in Hawaiʻi. *Pacific Science*, 305-324.

Sanderson, M. 1993. Introduction, in *Prevailing Trade Winds: Weather and Climate in Hawai'i*, edited by M. Sanderson, 1-11, Univ. of Hawai'i Press, Honolulu.

Schaetzl, Randall J., and Anderson, Sharon. *Soils: genesis and geomorphology*. Cambridge: Cambridge University Press, 2005. Print.

Selling, O.H. (1946). "Studies in Hawaiian Pollen Statistics. Part I. The Spores of the Hawaiian Pteridophytes." Bernice P. Bishop Museum Special Publication 37.

Selling, O.H. (1947). "Studies in Hawaiian Pollen Statistics. Part II. The Pollens of the Hawaiian Phanerograms." Bernice P. Bishop Museum Special Publication 38.

Selling, O.H. (1948). "Studies in Hawaiian Pollen Statistics. Part III. On the Late Quaternary History of the Hawaiian Vegetation." Bernice P. Bishop Museum Special Publication 39.

Sohmer, S. H., and Robert Gustafson. *Plants and flowers of Hawai'i*. Honolulu: University of Hawai'i Press, 1987. Print.

Stoermer, E.F., and Smol, J.P. 1999. The Diatoms: Applications for Environmental and Earth Sciences. *Cambridge University Press*. p. 469.

Sumner, M. E.. *Handbook of soil science*. Boca Raton, Fla: CRC Press, 2000. Print.

Tiunov, A.V. 2006. Stable Isotopes of Carbon and Nitrogen in Soil Ecological Studies. *Biology Bulletin* 34, 395-407.

Townsend, A.R. Vitousek, P.M., and Trumbore, S.E. 1995. Soil Organic Matter Dynamics Along Gradients in Temperature and Land Use on the Island of Hawai'i. *Ecology* 76(3), 721-733.

Uchikawa, J., Popp, B., Schoonmaker, J., Timmermann, A., and Lorenz, S. *in press*. 2010. Geochemical and climate modeling evidence for Holocene aridification in Hawai'i: dynamic response to a weakening equatorial cold tongue. *Quaternary Science Reviews*, doi: 10.1016/j.quascirev.2010.07.014.

Ulrich, Lüttge. *Physiological ecology of tropical plants*. Berlin: Springer, 1997. Print.

Wagner, W.L., Herbst, D.R., and Sohmer, S.H. (1990). Manual of the flowering plants of Hawai'i. Bishop Museum Press, Honolulu, Hawai'i.

Wang, Q., Li, Y., and Wang, Y. 2011. Optimizing the weight loss-on-ignition methodology to quantify organic and carbonate carbon of sediments from diverse sources. *Environ Monit Assess* 174, 241-257.

Wright, A.L., and Inglett, P.W. 2009. Soil and Carbon and Nitrogen and Distribution of Carbon-13 and Nitrogen-15 in Aggregates of Everglades Histosols. *Soil Science Society of America Journal* 73, 427-433.

Yu, Z., Campbell, I.D., Campbell, C., Vitt, D.H., Bond, G.C., and Apps, M.J. 2003. Carbon sequestration in western Canadian peat highly sensitive to Holocene wet-dry climate cycles at millennial timescales. The Holocene 13(6), 801-808.

Yu, Z., Loisel, L., Brosseau, D.P., Beilman, D.W., and Hunt, S.J. 2010. Global peatland dynamics since the Last Glacial Maximum. *Geophysical Research Letters* 37, L13402.

CHAPTER 4. CONCLUSIONS AND FUTURE DIRECTIONS

4.1 Summary

Drought conditions affect Hawaiʻi in areas such as water supply, agriculture, environment, and public health (Izuka 2006; Moncur 1989)). Recent droughts in Hawaiʻi have occurred in 1983-1984, 1996, the winters of 1997-2001 and 2006 during which parts of Hawaiʻi were designated primary natural disaster areas (Wilson 2005). Paleoclimate records from Kaʻau Crater reveal that precipitation can vary on millennial time scales; also, there have been periods of prolonged wet as well as dry climate, which may have caused decreased water table level. Now that humans depend on the water received at mountaintop locations, drought conditions have more serious consequences than vegetation change and peat dynamics.

Wetlands are important to the landscapes of the Hawaiian Islands. Historically, Hawaiʻi contained an estimated 59,000 acres of wetlands; however, Hawaiʻi has lost over 12 percent of its original wetland acreage (ELI 2008). Low lying wetlands such as riverine, found along rivers; estuarine, which occur on coasts where streams enter oceans; and marine, such as tide pools and sea grass beds, are all critical habitat areas for native flora and fauna in Hawaiʻi. Palustrine wetlands, such as montane marshes and bogs, are less common in Hawaiʻi, although are as important as lowland wetlands in terms of water collection, infiltration, and delivery of resources to downstream habitats. Montane wetlands are critical to preserve as they help store water during heavy rainfall, recharge aquifers and are zones of unique biodiversity. With the ever-growing global population and the accompanying demands, it is projected that water shortages and rights may become pressing societal dilemmas (Barlow 2008). This research demonstrates a dynamic relationship between rainfall and water table level at Kaʻau Crater. The crater water table level may rise quickly in response to increased rainfall, but has the capacity to drop in the absence of precipitation.

Vegetation composition throughout the Holocene in Kaʻau Crater also reveals plant adaptation patterns across dry to wet-tolerant taxa. As instances and severity of drought is predicted to increase in coming years, paleoclimate research will be essential in predicting ecological responses to climate changes. Research on Hawaiian wetlands increased with the passage of the Clean Water Act and implementing regulations in 1977 and the U.S. Endangered Species Act in 1973, nevertheless the majority of regulations and research pertain to lowlands wetlands (Scott 1993). By understanding historical patterns and functions of montane wetlands in Hawaiʻi, we may better prepare natural resource managers for scenarios such as enhanced drought conditions and decreased winter rainfall.

4.2 Future research

The presence of diatoms was recorded during pollen identification of the Kaʻau Crater core, which may also be used as a marker of moisture change in the crater. Diatoms are unicellular algae generally placed in the family Bacillariophyceae (Fig. 14). Diatoms are a major component of plankton, free-floating microorganisms of marine or freshwater systems (Round et al. 1990). The cell walls of these organisms are made of silica; hence fossils are often well preserved in lake and marine systems. In general, diatom species are very fastidious about the water chemistry in which they live. In particular, species have distinct ranges of pH and salinity where they will grow (Stoermer and Smol 1999). Diatoms also have ranges and tolerances for other environmental variables, including nutrient concentration, suspended sediment, flow regime, and elevation (Round et al. 1990). A considerable decrease in diatom abundance in the Kaʻau Crater record begins at approximately 5500 cal yr BP (Fig. 13e). The application of hydrofluoric acid during the pollen preparation procedure should have eliminated all diatoms; it is possible that variation between batches allowed for select diatoms to resist dissolution. Diatom abundance may therefore reflect altering procedural circumstances between batches. Change in diatom numbers throughout the core does however present and interesting configuration. Diatom richness remains low and variable until an increase around 4500 cal yr BP (Fig. 13e). Considering the specific preferences of diatoms, it is conceivable that there were mid-Holocene changes in the crater conditions possibly resulting from altered precipitation patterns that lead to diatom population alterations. Diatoms are commonly used as indicators of pollution in water based on diversity changes in diatom communities and species' tolerance to pollution. However, diatoms were not the focus of this study so further research could investigate diatom population dynamics in Kaʻau Crater (Michels 1998).

Over 450 wetlands including natural lakes, coastal marshes, mangrove swamps and upland bogs, have been identified across the main Hawaiian Islands, although the observation and protection of wetlands in Hawaiʻi are rather recent endeavors (Scott 1993). Prior to western contact, upland bogs, such as Kaʻau Crater were mildly used by Polynesian settlers compared to the lowland wetlands were. As agricultural practices and population began expanding, attempts at using upland areas as reservoirs were made such as that in Kaʻau Crater at the onset of the twentieth century. Mammals such as feral pigs, mongooses and rats were introduced to many Hawaiian Islands and spread to inhabit coastal areas to mountaintops, posing threats to wetland habitats (Stone 1988). Diverting streams and altering landscapes has been common in Hawaiʻi and undoubtedly will continue. Further research may focus on irreplaceable services, which montane wetlands provide not just for wildlife but for humans. Investigating paleo records of more upland areas across the main Hawaiian Islands would provide a framework for the general historic functional states of these areas thereby broadening the template upon which the present conditions may be compared.

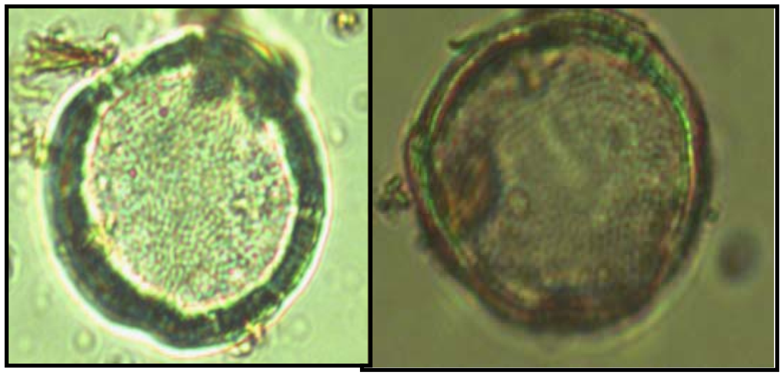

Fig. 15. Photographed diatoms from the Ka‘au Crater sediment core.

4.3 Literature cited

Barlow, Maude. *Blue covenant: the global water crisis and the coming battle for the right to water*. New York: New Press; 2008. Print.

Environmental Law Institute (ELI). 2008. State Wetland Protection: Status, Trends, and Model Approaches. A 50-state study by the ELI. U.S. Environmental Protection Agency.

Hawaiʻi's Wetlands: Mauka to Makai. 2009. (Report) State of Hawaiʻi Department of Land and Natural Resources, Division of Forestry and Wildlife, Pacific Coast Joint Venture.

Izuka, Scot K. 2006. Effects of Irrigation, Drought, and Ground-Water Withdrawals on Ground-Water Levels in the Southern Lihue Basin, Kauaʻi, Hawaiʻi. Scientific Investigations Report. U.S. Geological Survey. no. 2006-5291, 42 pp.

Michels, A. 1998. Use of Diatoms (Bacillariophyceae) for water quality assessment in two tropical streams in Costa Rica. *Rev. Biol. Trop.* 46, 143-152.

Moncur, J.E.T. 2007. Drought episodes management: the role of price. *JAWRA Journal of the American Water Resources Association* 25, 499-505.

Round, F.E., Crawford, R.M., and Mann, D.G. 1990. The Diatoms, Biology and Morphology of the Genera. *Cambridge University Press.* p. 747.

Scott, Derek A. *A Directory of wetlands in Oceania*. Slimbridge, U.K.: IWRB; 1993. Print.

Stoermer, E.F., and Smol, J.P. 1999. The Diatoms: Applications for the Environmental and Earth Sciences. *Journal of Phycol.* 35, 1340-1342.

Stone, Charles P. 1988. Hawaiʻi's Wetlands, Streams, Fishponds, and Pools. Ch. 29.

Wilson Okamoto Corporation Engineers and Planners. State of Hawaiʻi Department of Land and Natural Resources Commission on Water Resource Management. 2005. Hawaiʻi Drought Plan. Print.